Incipient loop-current order in the underdoped cuprate superconductors

Saheli Sarkar, Debmalya Chakraborty, and Catherine Pépin
Institut de Physique Théorique, Université Paris-Saclay, CEA, CNRS, F-91191 Gif-sur-Yvette, France

(Received 26 June 2019; revised manuscript received 19 November 2019; published 30 December 2019)

There is growing experimental evidence that indicates discrete symmetry-breaking-like time-reversal ($\mathcal{T}$), parity ($\mathcal{P}$), and C_4 lattice rotation in the pseudogap state of underdoped copper-oxide-based (cuprate) superconductors. The discrete symmetry breaking manifests a true phase transition to an ordered state. A detailed thermodynamic understanding of these orders can answer various puzzles related to the nature of the transition at the pseudogap temperature T^*. In this work, we investigate the thermodynamic signature of $\mathcal{T}$-$\mathcal{P}$ symmetry breaking considering superconductivity (SC) and bond-density wave (BDW) as two primary orders. The BDW can generate both modulating charge and current densities. This framework takes into account an intricate competition between the ubiquitous charge density wave and SC, which is prominent in various cuprates in the underdoped regime. We demonstrate that within the mean-field approach of competing BDW and SC orders, a $\mathcal{T}$-$\mathcal{P}$ breaking ground state of coexisting BDW and SC can be stabilized, provided the BDW itself breaks $\mathcal{T}$-$\mathcal{P}$. But this ground state ceases to occur at higher temperatures. However, we show that fluctuations in SC and BDW can bring about the emergence of an unusual translational symmetry preserving order due to a preemptive phase transition by spontaneously breaking $\mathcal{T}$-$\mathcal{P}$ at a higher temperature before the primary orders set in. We refer to this order as magnetoelectric loop current (MELC) order. We present the possible nature of the phase transition for this incipient MELC order and discuss some experimental relevance.

DOI: 10.1103/PhysRevB.100.214519

I. INTRODUCTION

The various anomalies in the normal-state properties of the underdoped regime of hole-doped cuprate superconductors have been a long-standing puzzle in condensed-matter physics. This peculiar normal state has a partially gapped Fermi surface and is known as a "pseudogap" (PG) state. The PG state [1–13] for the underdoped cuprates is usually set below a characteristic temperature T^* well above the superconducting critical temperature T_c as indicated in several experiments. Whether the PG state appears through a true phase transition at T^* associated with symmetry breaking is still a matter of debate. A complete understanding of the nature of this transition and the corresponding broken symmetries can unravel the mystery of the PG state.

Several experiments have provided evidence of a true phase transition at T^* and various examples of symmetry breaking in the PG state. Ultrasound spectroscopy [14] and magnetic quantum oscillation measurements [15] showed signatures of a thermodynamic phase transition at T^*. Moreover, recent experiments suggest a breaking of discrete ($\mathbb{Z}_2$) symmetries in the PG state, which makes it intriguing to associate the discrete symmetry breaking with the phase transition at T^*. Angle-resolved photoemission spectroscopy (ARPES) with circularly polarized photons for underdoped $Bi_2Sr_2CaCu_2O_{8+\delta}$ (BSCCO) [16] in the PG state suggested time-reversal symmetry breaking (Fig. 1). Spin-polarized neutron scattering in $YBa_2Cu_3O_{6+x}$ (YBCO) [17,18], $HgBa_2CuO_{4+\delta}$ [19,20], and $Bi_2Sr_2CaCuO_{8+\delta}$ [21] have shown evidence of long-range magnetic order at T^* with wave-vector $\vec{Q}=0$. This magnetic order preserves lattice translational invariance but breaks the time-reversal symmetry. Another spin polarized neutron scattering [22] in $La_{2-x}Sr_xCuO_4$ has reported short-range magnetic order. Optical second-harmonic-generation (OSHG) measurement [23] suggested breaking of parity symmetry at T^* (Fig. 1). Apart from these, polar Kerr effect measurements showed finite rotation of linearly polarized light reflected from the sample within the PG state in a number of underdoped cuprates [24–26]. The Kerr effect observations were interpreted in terms of time-reversal symmetry breaking [27] and sometimes in terms of chiral symmetry breaking [28–30]. Scanning tunneling microscopy (STM) [31,32], the anomalous Nernst effect [33], torque magnetometry [34], and polarized neutron diffraction measurement [35] have also detected nematic order inside the PG state, which breaks the lattice C_4 rotational symmetry down to C_2, but preserves lattice translational symmetry and hence is a $\vec{Q}=0$ order.

Signatures of time-reversal ($\mathcal{T}$) symmetry breaking from polarized neutron scattering experiments in different cuprate compounds [17,19,21,22] motivated several theoretical studies. Varma *et al.* [36–39] first proposed the origin of $\mathcal{T}$ breaking $\vec{Q}=0$ magnetic moments in the polarized neutron scattering in the PG state due to the existence of intra-unit-cell (IUC) loop currents. The IUC currents preserve lattice translational symmetry as they exist inside a single unit cell. The loop currents additionally break parity ($\mathcal{P}$) symmetry explaining the features of OSHG experiment [40]. The IUC loop currents proposed by Varma require a three-band model of CuO_2 planes. The possibility of such currents in three-band microscopic models was further explored in several theoretical works [41–46]. However, numerical analysis [47,48] and quantum variational Monte Carlo study [49] have challenged the existence and stability of such currents.

Furthermore, a nonsuperconducting $\vec{Q}=0$ order is not expected to open a gap on the Fermi surface, as it can either

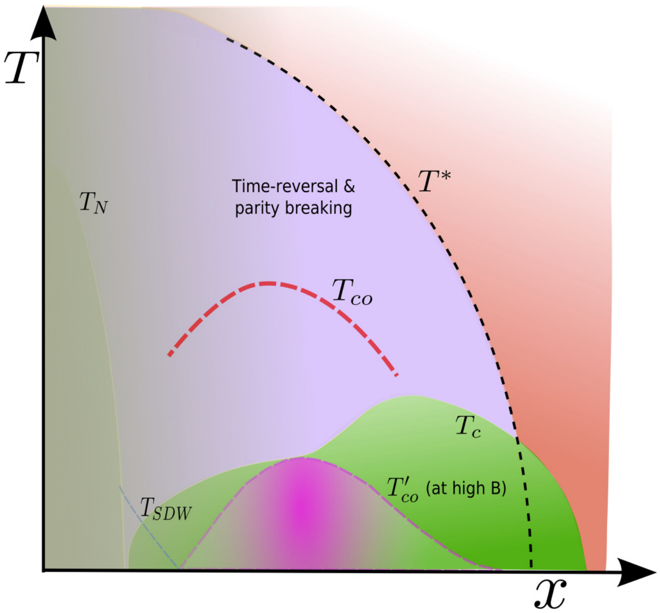

FIG. 1. A schematic temperature (T) hole doping (x) phase diagram of cuprates summarizing experiments. Upon small doping, the system exhibits a d-wave superconducting phase below the critical temperature T_c that follows a domelike shape. A mysterious PG state appears below a temperature T^*, which is much higher than T_c in the underdoped region. Different experiments observed time-reversal and parity symmetry breaking in the PG state. A short-range CO is seen below T_{CO}, whereas CO becomes long-range upon application of a magnetic field below temperature T'_{CO}.

change the dispersion of the quasiparticle spectrum or it can simply shift the chemical potential. Additionally, it cannot explain the presence of various $\vec{Q} \neq 0$ orders at low temperatures. These indicate that finite $\vec{Q}$ orders become imperative to open a gap on the Fermi surface, and indeed such orders have been observed in experiments. X-ray diffraction [50–58] and STM [59–62] ubiquitously detected charge-density-wave order (CO) for $T < T_{\mathrm{CO}}$ (Fig. 1). The CO breaks lattice translational symmetry and consequently has finite wave vector ($\vec{Q} \neq 0$). There are also experimental indications [32,53,63–65] that the modulations of the charge density live primarily on Cu-O-Cu bonds. In the presence of a high magnetic field, the CO attains a long-range nature in YBCO [66–72] below T'_{CO} (Fig. 1). It is also interesting to note that various experiments [50,54,59,73,74] observed a competition between CO and SC. More recently, local Josephson scanning tunneling microscopy provided evidence of a distinct finite $\vec{Q}$ electronic order, namely a pair-density-wave (PDW) [75–77] in BSCCO [74,78].

Although there are no signatures of long-range finite $\vec{Q}$ orders close to T^*, experiments hint at the presence of various fluctuations. This motivated several theoretical proposals on fluctuations of different order parameters driving the phenomenology of the PG state. Proximity to the Mott localization transition [79] inspired scenarios with superconducting phase fluctuations [80,81] and fluctuating preformed Cooper pairs [82–84]. On the other hand, the presence of various competing orders [85,86] in the underdoped region of the phase diagram led to theories with fluctuations in various orders such as spin density waves [87,88], staggered flux phase [89,90], CO [91–93], and PDW [94–97]. There are also proposals based on fluctuations guided by an emergent symmetry [91,92,98]. The emergent SU(2) theory describes some of the phenomenology [99–108] for the PG phase. Recent experimental signatures of fluctuations in both SC [109–111] and charge [112] channels in the PG state motivated a theoretical proposal [113] for a pseudogap based on entangled fluctuating preformed particle-particle and particle-hole pairs. While particle-particle pairs result in the SC state, the particle-hole pairs give rise to bond-density-wave (BDW) order, which can result in both charge-density-wave order and current-density-wave order.

Fluctuating orders can also be considered as possible candidates for explaining the antinodal gap on the Fermi surface in the PG phase. For instance, superconducting fluctuations can result in Fermi arcs as observed in ARPES for $T > T_c$ because the nodal quasiparticles are more prone to thermal fluctuations than the antinodal ones [114]. Within the fluctuation scenarios, therefore, it is of fundamental importance to investigate discrete symmetry breaking $\vec{Q} = 0$ orders close to temperature T^* and their connection to the PG transition. Some phenomenological works [93,115] discussed discrete symmetry breaking in the PG state using composite CO and PDW fields. But no general consensus as to whether these theoretical frameworks can consolidate the mechanism of a pseudogap and discrete symmetry-breaking orders has been reached so far.

In this paper, we are interested in whether fluctuations in both SC and BDW hold the key to the $\mathcal{T}$-$\mathcal{P}$ symmetry breaking in the PG state resulting in a phase transition at T^*. Toward this end, we first investigate a Ginzburg-Landau (GL) theory of competing primary BDW and SC orders at the mean-field level without considering fluctuations. We notice that $\mathcal{T}$-$\mathcal{P}$ symmetry can only be broken in a coexisting ground state of SC and BDW, where BDW itself breaks $\mathcal{T}$-$\mathcal{P}$ symmetry. Such a ground state has never been observed in experiments. This immediately raises the possibility of a role played by the fluctuations in the SC and BDW. To analyze the effect of fluctuations, we construct a composite PDW order from higher-order combinations of primary SC and BDW orders. The composite PDW order has the same wave vector $\vec{Q}$ as that of BDW and has the same charge as SC. The fluctuations in both SC and BDW lead to the fluctuations in composite PDW order. Using a Hubbard-Stratonovich (HS) method with a saddle-point approximation in a GL theory of fluctuating composite PDW order, we find a nontrivial order that can break $\mathcal{T}$-$\mathcal{P}$ in the PG state. In our phenomenological treatment, the $\mathcal{T}$-$\mathcal{P}$ symmetry breaking order parameter shares the same symmetry properties as those of the IUC magnetoelectric loop current (MELC) proposed by Varma. Hence, we refer to this order parameter as MELC order in the rest of this paper. However, the MELC order in our theory is an emergent $\vec{Q} = 0$ order, formed by a higher-order combination of primary SC and BDW, and thus does not need resorting to the three-band models.

We organize the rest of the paper as follows. In Sec. II we define the two primary order parameters, SC and BDW, and we construct a composite PDW order parameter. We discuss in detail the symmetry properties of the order parameters in the

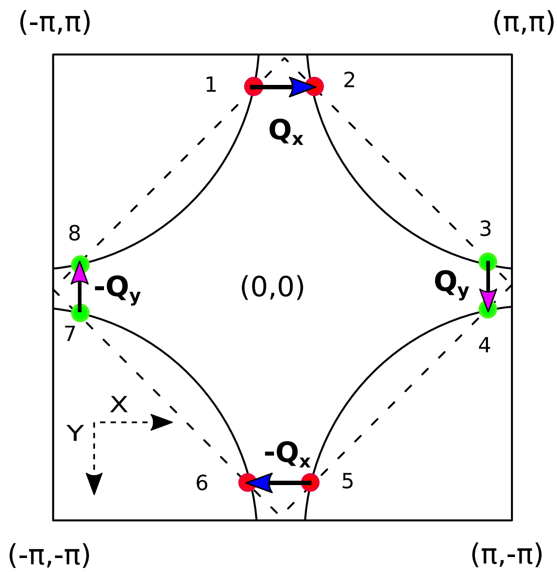

FIG. 2. A schematic representation of the Fermi surface of hole-doped cuprates. The dotted lines represent the magnetic Brillouin zone boundary and the solid curved lines denote the Fermi surface. The Fermi surface intersects the magnetic Brillouin zone boundary at eight hot-spots, which are shown by red and green dots and numbered from 1 to 8. As mentioned in the text, we consider the BDW order parameters with axial wave vectors connecting the nearest hot spots in the first Brillouin zone. The BDW wave vectors for hot spots 1, 3, 5, and 7 are shown by the arrows. For orthorhombic lattice systems, BDW order parameters corresponding to only the red hot-spots are relevant. On the other hand, for tetragonal lattice systems, BDW order parameters corresponding to both red and green hot spots have to be considered for writing the free energy.

context of cuprates. In Sec. III we build an auxiliary MELC order parameter and discuss its symmetry transformation properties. In Sec. IV we present the mean-field GL theory of competing SC and BDW and we calculate the analytic conditions for obtaining the $\mathcal{T}$-$\mathcal{P}$ breaking ground state. In Sec. V we present the HS approach for fluctuations and we detail the possible nature of the phase transition depending on parameters through which the preemptive MELC ground state can appear. In Sec. VI we put forward discussions on the extensions of the framework and possible relevance to experimental findings in cuprates. In Sec. VII we conclude by presenting a summary of our work.

II. ORDER PARAMETERS: SYMMETRY PROPERTIES

In this section, we introduce the Fermi surface (Fig. 2) and the order parameters of a typical hole-doped cuprate. More specifically, we discuss here two primary order parameters—BDW and SC—and the secondary order parameter, composite PDW, and their symmetry transformation properties.

Underdoped cuprates [91,116] are often described by a spin-fermion model [117–119] based on antiferromagnetic fluctuations. Within this scenario, the PG phase is described by an emergent symmetry between the SC order and a BDW order with diagonal wave vectors connecting different "hot-spots" (labeled as 1–8 in Fig. 2), where the Fermi surface intersects the magnetic Brillouin zone boundary [91]. But experimentally the CO is observed with wave vectors either horizontal or vertical to the crystallographic axes [58,120]. The magnitude of the wave vector is found to be very close to the axial wave vector connecting two neighboring hot-spots [120]. Theoretically, BDW with axial wave vectors can also be obtained as one of the competing instabilities in models with antiferromagnetic fluctuations [93]. The BDW with an axial wave vector can be enhanced by including fluctuations [93,100,103], considering dynamic exchange interactions [121], or an off-site Coulomb interaction [122] in the microscopic models. Furthermore, a recent work [113] including both antiferromagnetic interactions and off-site Coulomb repulsion shows that a BDW with an axial wave vector dominates near the hot-spots on the Fermi surface. Motivated by all these theoretical indications and experimental observations, we consider the BDW order parameter only at the hot-spots with axial wave vectors ($\vec{Q}_x$ or $\vec{Q}_y$) as shown in the Fig. 2.

The complex BDW order parameter χ_Q^k with ordering wave vector $\vec{Q}$ at each given momentum (k) is given as $\sum_\sigma \langle c^\dagger_{k+Q,\sigma} c_{k,\sigma}\rangle$. In the special case where χ_Q^k describes only current modulations with $Q = (\pi,\pi)$, the corresponding order parameter is often referred to as d-density waves (dDW) [123] or staggered flux order parameters [124–126] in the literature. While the dDW ground state itself breaks $\mathcal{T}$-$\mathcal{P}$ [123], the BDW ground state considered in this paper does not necessarily break $\mathcal{T}$-$\mathcal{P}$, as we will see in Secs. IV and V (also see Ref. [93]).

The complex superconducting order parameter Δ is given by $\langle c^\dagger_{k,\uparrow} c^\dagger_{-k,\downarrow}\rangle$. Next we introduce the PDW order parameter, which is a composite of χ_Q^k and Δ and can be defined as

$$\Phi_Q^k = \chi_Q^k \Delta. \tag{1}$$

We would like to emphasize that the wave vector of the PDW order Φ_Q^k is the same as that of the BDW wave vector. A different set of theories [94,95,127,128] considered fluctuating primary PDW, albeit with a different wave vector $\vec{P}$ from that of the CO wave vector.

For tetragonal crystal systems, all the hot-spot pairs (1-2, 3-4, 5-6, and 7-8) need to be considered because of C_4 symmetry in the system. In this case, there are eight complex BDW order parameters for each hot-spot point. For orthorhombic systems, the relevant hot-spot pairs are 1-2 and 5-6 as the C_4 symmetry is now absent and one cannot bring 1-2 and 5-6 pairs to any of the hot-spot pairs 7-8 or 3-4. Therefore, in the orthorhombic case, there are four complex order parameters corresponding to the hot-spot points 1, 2, 5, and 6 (shown with red dots in Fig. 2). The complex order parameters for orthorhombic system, corresponding to the primary order manifold, are

$$[\chi^1_{Q_x}, \chi^2_{-Q_x}, \chi^5_{-Q_x}, \chi^6_{Q_x}, \Delta]. \tag{2}$$

To build the Ginzburg-Landau free energy density, the point-group symmetry transformation properties of these order parameters are required. For the orthorhombic case, the required point group symmetries are as follows: three twofold axes of rotations about the x, y, and z axis, and three mirror planes: $y-z$, $z-x$, and $x-y$. We are interested only in the parity and (or) time-reversal symmetry breaking. Thus, we do not consider any mirror symmetry breaking ground states. As a result, without any loss of generality, we implement the

TABLE I. Point-group symmetry transformation of SC, BDW, and PDW fields in an orthorhombic lattice. Here R_x, R_y, and R_z represent the action of the twofold (C_2) rotations about the x, y, and z axes, respectively. σ_x, σ_y, and σ_z represent the action of mirror reflections about the y-z, z-x, and x-y planes, respectively.

Point-group	Primary orders			Composite orders	
operations	χ_Q^k	χ_{-Q}^{-k}	Δ	Φ_Q^k	Φ_{-Q}^{-k}
R_x:	χ_Q^k	χ_{-Q}^{-k}	Δ	Φ_Q^k	Φ_{-Q}^{-k}
R_y:	χ_{-Q}^{-k}	χ_Q^k	Δ	Φ_{-Q}^{-k}	Φ_Q^k
R_z:	χ_{-Q}^{-k}	χ_Q^k	Δ	Φ_{-Q}^{-k}	Φ_Q^k
σ_x:	χ_{-Q}^{-k}	χ_Q^k	Δ	Φ_{-Q}^{-k}	Φ_Q^k
σ_y:	χ_Q^k	χ_{-Q}^{-k}	Δ	Φ_Q^k	Φ_{-Q}^{-k}
σ_z:	χ_Q^k	χ_{-Q}^{-k}	Δ	Φ_Q^k	Φ_{-Q}^{-k}

following two equalities:

$$\chi_{Q_x}^1 = \chi_{Q_x}^6 \equiv \chi_Q^1,$$
$$\chi_{-Q_x}^5 = \chi_{-Q_x}^2 \equiv \chi_{-Q}^5. \tag{3}$$

Subsequently, the order parameter space is further reduced to a smaller subset,

$$\left[\chi_Q^1, \chi_{-Q}^5, \Delta\right]. \tag{4}$$

Rewriting χ_Q^1 and χ_{-Q}^5 as χ_Q^k and χ_{-Q}^{-k}, respectively, the order parameter manifold becomes

$$\left[\chi_Q^k, \chi_{-Q}^{-k}, \Delta\right]. \tag{5}$$

Finally, we summarize the point group symmetry transformation of the BDW, SC, and composite PDW in Table I. The order parameter manifold for the tetragonal lattice systems will be larger than in Eq. (4) and the number of possible ground states will be increased. While we explicitly show the order parameter manifold and discuss the case for tetragonal systems in Sec. VI A, we will restrict the analysis in the rest of this paper to orthorhombic lattice systems with no mirror symmetry breaking order parameters in order to have analytical control in a reduced parameter space.

Under parity and time-reversal, the BDW and the composite PDW transform as follows:

$$\chi_Q^k \xrightarrow{\mathcal{P}} \chi_{-Q}^{-k},$$
$$\chi_Q^k \xrightarrow{\mathcal{T}} \chi_{-Q}^{\dagger -k},$$
$$\Phi_Q^k \xrightarrow{\mathcal{P}} \Phi_{-Q}^{-k},$$
$$\Phi_Q^k \xrightarrow{\mathcal{T}} \Phi_{-Q}^{\dagger -k}. \tag{6}$$

For convenience from now on we will suppress the k index from the BDW order parameters. For example, we will use χ_Q and χ_{-Q} for χ_Q^k and χ_{-Q}^{-k} respectively. The same notation will also be applied to the composite PDW.

III. LOOP CURRENT ORDER

Our goal in this work is to study $\mathcal{T}$-$\mathcal{P}$ symmetry breaking due to the emergence of an order in the PG state. Here, we define such an order parameter, referred to as MELC order, which is translationally invariant ($\vec{Q} = 0$). Within our theoretical framework, this order appears to be an auxiliary order. The concept of auxiliary orders has been introduced previously in several contexts [46,85,93,115,129], and sometimes they are referred to as "vestigial" or "secondary" orders.

In a similar spirit, we construct the MELC order parameter ℓ from the primary BDW and SC order parameters, and it is given by the following equation:

$$\ell = |\chi_Q\Delta|^2 - |\chi_{-Q}\Delta|^2. \tag{7}$$

Equivalently, ℓ can be written in terms of the composite PDW order parameters using Eq. (1) as follows:

$$\ell = |\Phi_Q|^2 - |\Phi_{-Q}|^2. \tag{8}$$

Upon time-reversal and parity transformation, the BDW and composite PDW transform as given by Eq. (6). Using Eq. (6), ℓ transforms under time-reversal and parity as

$$\ell \xrightarrow{\mathcal{T}} -\ell, \quad \ell \xrightarrow{\mathcal{P}} -\ell, \quad \ell \xrightarrow{\mathcal{TP}} \ell. \tag{9}$$

This shows that the order parameter ℓ breaks the time-reversal parity but preserves their product. Under a spatial translation by $\vec{R}$, χ_Q and Φ_Q transform as $\chi_Q \to e^{i\vec{Q}\cdot\vec{R}}\chi_Q$ and $\Phi_Q \to e^{i\vec{Q}\cdot\vec{R}}\Phi_Q$, respectively. Hence ℓ remains invariant under a spatial translation $\vec{R}$ and therefore is a $\vec{Q} = 0$ order. Magnetoelectric IUC loop currents proposed by Varma [36] also have similar transformation properties under time-reversal, parity, and spatial translation.

IV. MEAN-FIELD GINZBURG-LANDAU THEORY OF SC AND BDW

This section aims to investigate the formation of the MELC order by constructing a mean-field Ginzburg-Landau theory of competing BDW and SC orders. The GL free energy density functional for a spatially homogeneous case, which remains invariant under translations, time-reversal, parity, gauge symmetries, as well as all the point group symmetry operations of the orthorhombic system, is given as follows:

$$\begin{aligned} F = {} & \alpha_d|\Delta|^2 + \alpha(|\chi_Q|^2 + |\chi_{-Q}|^2) \\ & + \frac{\beta_1}{2}(|\chi_Q|^4 + |\chi_{-Q}|^4) + \frac{\beta_d}{2}|\Delta|^4 \\ & + \beta_2(|\chi_Q|^2|\Delta|^2 + |\chi_{-Q}|^2|\Delta|^2) + \beta_3(|\chi_Q|^2|\chi_{-Q}|^2) \\ & + \beta_4[\chi_Q\chi_{-Q}|\Delta|^2 + |\Delta|^2(\chi_Q\chi_{-Q})^*]. \end{aligned} \tag{10}$$

In the free energy Eq. (10), β_2 gives the coupling between BDW field χ_Q or χ_{-Q} and superconducting field Δ. β_3 represents coupling between χ_Q and χ_{-Q}. And lastly, β_4 gives the mutual coupling between the three fields χ_Q, χ_{-Q}, and Δ. In this work, we are particularly interested in a ground state that spontaneously breaks only $\mathcal{T}$-$\mathcal{P}$ symmetry and can sustain a MELC. Subsequently we replace $\beta_4 = 0$ in the free energy density for simplification, which excludes the possibilities of pure imaginary ground states.

A. All possible ground states

We now discuss the possible mean-field ground states of SC and BDW orders from the free energy Eq. (10). The

TABLE II. Properties of all possible mean-field ground states. The nonzero values of χ_Q and χ_{-Q} in the first two columns are the same as the free energy density Eq. (10) is invariant under $\chi_Q \leftrightharpoons \chi_{-Q}$. The fourth column shows the symmetries broken by the corresponding ground state of the primary orders. The fifth column gives the free energy for each state. The last three columns show the composite PDW order and the MELC order constructed from the primary orders. Only states $(a, 0, b)$ and $(0, a, b)$ can sustain a nonzero value of the MELC order.

Primary orders			Broken symmetry	Free energy	Composite PDW		MELC
χ_Q	χ_{-Q}	Δ	in the ground state		Φ_Q	Φ_{-Q}	ℓ
a	0	b	$U(1)\times U(1)\times\mathbb{Z}_2$	$F(a,0,b)=\frac{[2\alpha\alpha_d\beta_2-\alpha_d^2\beta_1-\alpha^2\beta_d]}{2[\beta_1\beta_d-\beta_2^2]}$	ab	0	a^2b^2
0	a	b	$U(1)\times U(1)\times\mathbb{Z}_2$	$F(0,a,b)=\frac{[2\alpha\alpha_d\beta_2-\alpha_d^2\beta_1-\alpha^2\beta_d]}{2[\beta_1\beta_d-\beta_2^2]}$	0	ab	$-a^2b^2$
a	a	b	$U(1)\times U(1)$	$F(a,a,b)=\frac{4\alpha\alpha_d\beta_2-\alpha_d^2(\beta_1+\beta_3)-2\alpha^2\beta_d}{2\beta_d(\beta_1+\beta_3)-4\beta_2^2}$	ab	ab	0
a	0	0	$U(1)\times\mathbb{Z}_2$	$F(a,0,0)=\frac{-\alpha^2}{2\beta_1}$	0	0	0
0	a	0	$U(1)\times\mathbb{Z}_2$	$F(0,a,0)=\frac{-\alpha^2}{2\beta_1}$	0	0	0
0	0	b	$U(1)$	$F(0,0,b)=\frac{-\alpha_d^2}{2\beta_d}$	0	0	0
a	a	0	$U(1)$	$F(a,a,0)=\frac{-\alpha^2}{(\beta_1+\beta_3)}$	0	0	0

calculations to obtain the solutions for the ground states by minimizing the free energy Eq. (10) and the resulting free energy of the respective ground states are shown in Appendix. Table II summarizes the seven possible mean-field ground states of the free energy Eq. (10) and the free energy for each ground state. For $\alpha < 0$ and $\beta_1 > 0$, the state $(a, 0, 0)$ becomes a minimum, where the field χ_Q condenses with $\chi_Q \neq 0$. The superconducting state $(0, 0, b)$ becomes a minimum with $\Delta \neq 0$ when $\alpha_d < 0$, and $\beta_d > 0$. We note that there can be another BDW state $(a, a, 0)$ present, when both χ_Q and χ_{-Q} are nonzero and superconducting order parameter is absent. These two fields condense when $\alpha < 0$ and $(\beta_1 + \beta_3) > 0$.

We note in Table II that the two states $(a, 0, b)$ and $(0, a, b)$, where $|\chi_Q| \neq |\chi_{-Q}|$, have a $\mathbb{Z}_2$ degeneracy as their free energies are equal. This degeneracy can be lifted by spontaneously breaking the $\mathcal{T}$-$\mathcal{P}$ symmetry, and such a state will sustain a finite MELC, as can be seen from the last column of the table. No other states can sustain a finite MELC, which can also be seen from the table. Henceforth, we analyze the conditions on the GL parameters for the state $(a, 0, b)$ to be the most stable ground state.

B. Stability conditions for the $(a, 0, b)$ ground state

Now we analyze the stability for the state $(a, 0, b)$. The ground state $(a, 0, b)$ has a free energy,

$$F(a,0,b) = \frac{\left[2\alpha\alpha_d\beta_2 - \alpha_d^2\beta_1 - \alpha^2\beta_d\right]}{2\left[\beta_1\beta_d - \beta_2^2\right]}. \tag{11}$$

The stability conditions are essentially the conditions for which the state $(a, 0, b)$ is a global minimum. These conditions are given by

$$F(a,0,b) - F(a,a,b) < 0, \tag{12a}$$
$$F(a,0,b) - F(a,0,0) < 0, \tag{12b}$$
$$F(a,0,b) - F(0,0,b) < 0, \tag{12c}$$
$$F(a,0,b) - F(a,a,0) < 0. \tag{12d}$$

Thus the stable ground state is achieved by the simultaneous fulfillment of the above conditions provided all the other minima of the GL free energy exist. The minimum requirements for the existence of all the minima are $\alpha < 0$, $\alpha_d < 0$, $\beta_1 > 0$, $\beta_1 + \beta_3 > 0$, and $\beta_d > 0$, which we derived in Sec. IV A. These conditions for the parameters will be valid for the rest of the discussion in this section.

A close inspection of the comparison of free energies [Eqs. (12a), (12b), (12c), and (12d)] will also provide insight on the strength of relative couplings between various fields. Toward this end, we first evaluate the condition for which Eq. (12b) holds. This imposes the following additional constraint on the coupling constant β_2:

$$\left(\beta_2^2 - \beta_1\beta_d\right) < 0 \tag{13}$$

and it imposes two more conditions on the masses:

$$\beta_2\alpha_d > \alpha\beta_d \tag{14}$$

and

$$\alpha\beta_2 > \alpha_d\beta_1. \tag{15}$$

From Eq. (12c), we get the same criteria as those of Eqs. (14) and (15). The condition Eq. (12d) gives

$$2(\beta_1+\beta_3)\left(2\alpha\alpha_d\beta_2 - \alpha_d^2\beta_1 - \alpha^2\beta_d\right) > 2\alpha^2\left(\beta_1\beta_d - \beta_2^2\right). \tag{16}$$

Finally, we investigate the stability criteria Eq. (12a). The free energy density for the state (a, a, b) is given by

$$F(a,a,b) = \frac{4\alpha\alpha_d\beta_2 - \alpha_d^2(\beta_1+\beta_3) - 2\alpha^2\beta_d}{2\beta_d(\beta_1+\beta_3) - 4\beta_2^2}. \tag{17}$$

We notice from the free energy density Eq. (17) that there are two conditions for the state (a, a, b) to become one of the possible minima, i.e., $F(a, a, b) < 0$. The two conditions are given by the following equations:

$$2\beta_d(\beta_1+\beta_3) - 4\beta_2^2 < 0, \tag{18a}$$
$$4\alpha\alpha_d\beta_2 - \alpha_d^2(\beta_1+\beta_3) - 2\alpha^2\beta_d > 0, \tag{18b}$$

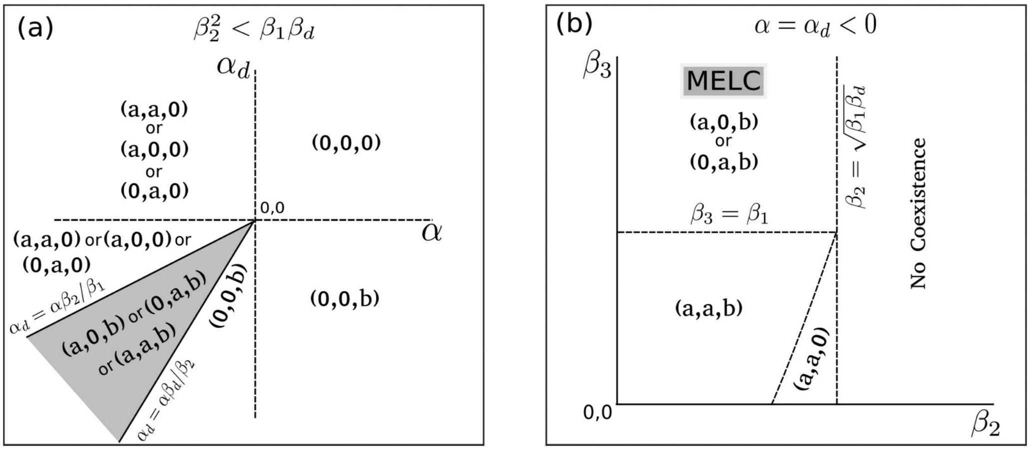

FIG. 3. Phase diagrams showing the parameter regimes for the occurrence of a MELC ground state obtained from the mean-field solutions of the GL free energy Eq. (10). (a) Illustration of different phases in the parameter space of α and α_d: We choose $\beta_2^2 < \beta_1\beta_d$ as it is a necessary condition for the coexistence of SC and BDW orders. For any positive values of both α and α_d, the system is in a disordered state (0, 0, 0). If $\alpha_d < 0$ and $\alpha > 0$, the only possible ground state is an SC state $(0, 0, b)$. If $\alpha_d > 0$ and $\alpha < 0$, the possible ground states are $(a, a, 0)$, $(a, 0, 0)$, and $(0, a, 0)$, where SC order vanishes and only BDW orders exist. When both $\alpha_d < 0$ and $\alpha < 0$, coexistent states of SC and BDW orders emerge as indicated by the gray-colored region. This region of coexistence is bounded by two lines obtained from Eqs. (14) and (15). There are three possible coexistent states: $(a, 0, b)$, $(0, a, b)$, and (a, a, b). However, only $(a, 0, b)$ or $(0, a, b)$ support a MELC order. (b) Role of the GL parameter β_3: With a choice of $\alpha = \alpha_d < 0$ [inside the gray region in (a)], the MELC ground state is found to be bounded below by $\beta_3 = \beta_1$. It is also seen that when $\beta_3 < \beta_1$, the state (a, a, b) wins over the MELC ground state, as a lower value of β_3 favors the existence of two BDW orders χ_Q and χ_{-Q}. Also the existence of state $(a, a, 0)$ is found from comparing free energies of state (a, a, b) and $(a, a, 0)$. In the parameter regime of $\beta_2 > \sqrt{\beta_1\beta_d}$, no coexistence of BDW and SC orders can be found.

or

$$2\beta_d(\beta_1 + \beta_3) - 4\beta_2^2 > 0, \tag{19a}$$

$$4\alpha\alpha_d\beta_2 - \alpha_d^2(\beta_1 + \beta_3) - 2\alpha^2\beta_d < 0. \tag{19b}$$

For the state $(a, 0, b)$ to become more stable than the state (a, a, b), the condition Eq. (12a) has to be satisfied. This poses an additional constraint,

$$2(\beta_1\beta_d - \beta_2^2)\left[4\alpha\alpha_d\beta_2 - \alpha_d^2(\beta_1 + \beta_3) - 2\alpha^2\beta_d\right] < \left[2(\beta_1 + \beta_3)\beta_d - 4\beta_2^2\right](2\alpha\alpha_d\beta_2 - \alpha_d^2\beta_1 - \alpha^2\beta_d), \tag{20}$$

on the masses and coupling constants in the free energy Eq. (10).

In Fig. 3, we present phase diagrams showing all the possible ground states and highlight the parameter regime where a ground state sustaining the MELC order is stable. As already indicated earlier in this section, only a state with coexisting SC and BDW fields can give rise to the MELC order. From Eq. (13), such a state is allowed only when $\beta_2^2 < \beta_1\beta_d$. Restricting β_2 in this regime, in Fig. 3(a) we plot the phase diagram in the parameter space of α and α_d. The three possible coexistent states—$(a, 0, b)$, $(0, a, b)$, and (a, a, b)—are stable only in the gray region as shown in Fig. 3(a). But as we saw in Table II, ℓ can have a nonzero value only for $(a, 0, b)$ and $(0, a, b)$. This imposes a further condition on other GL parameters. To further illustrate, we consider a particular line $\alpha = \alpha_d < 0$ in the gray region of Fig. 3(a) and we investigate the GL parameter β_3 in Fig. 3(b). We find that $(a, 0, b)$ and $(0, a, b)$ are stable when $\beta_3 > \beta_1$.

However, the two states $(a, 0, b)$ and $(0, a, b)$ have a $\mathbb{Z}_2$ degeneracy due to the presence of $\mathcal{T}$-$\mathcal{P}$ symmetry. Subsequently, the ground states of composite PDW also have the same $\mathbb{Z}_2$ degeneracy. This degeneracy can be lifted if the BDW itself spontaneously breaks $\mathcal{T}$-$\mathcal{P}$ symmetry. As a consequence, the $\mathcal{T}$-$\mathcal{P}$ broken ground state will have a finite MELC order, as can be seen from Eq. (7).

V. FLUCTUATING ORDERS AND PREEMPTIVE MELC ORDER

The $\mathcal{T}$-$\mathcal{P}$ breaking mean-field BDW ground state, which we discussed in Sec. IV, has not yet been observed, and such a ground state cannot persist at higher temperatures. This raises the possibility of a role played by fluctuations in $\mathcal{T}$-$\mathcal{P}$ breaking. In this section, we therefore analyze fluctuation effects of BDW and SC on $\mathcal{T}$-$\mathcal{P}$ breaking in the PG state.

The fluctuations in both BDW and SC introduce gradient terms of both SC and BDW orders in the GL free energy Eq. (10). This gives rise to additional parameters in the free energy Eq. (10). As a result, it becomes more complex to study the free energy analytically. But, we recall from Sec. III that the MELC order parameter is defined as $\ell = |\chi_Q\Delta|^2 - |\chi_{-Q}\Delta|^2$, where the $\chi_Q\Delta$ and $\chi_{-Q}\Delta$ are simply two composite PDW fields Φ_Q and Φ_{-Q}, respectively. Hence to investigate the $\mathcal{T}$-$\mathcal{P}$ breaking, alternatively we can write the free energy in terms of fluctuating composite PDW order parameters. This allows us to perform a systematic analytical study of the $\mathcal{T}$-$\mathcal{P}$ symmetry breaking in the PG state. The free energy in terms of fluctuating PDW orders will have the same symmetry properties as that of free energy in terms of SC and BDW in Sec. IV, as PDW and BDW transform in the exact same fashion under all symmetry transformations discussed in Sec. II.

Before considering the fluctuations, we write the GL free energy for the composite PDW in a homogeneous system, incorporating all the symmetries for a disordered normal state of the system. The corresponding free energy is given by

$$F_0[\Phi_Q, \Phi_{-Q}] = \alpha_\phi(|\Phi_Q|^2 + |\Phi_{-Q}|^2) + \beta_\varrho(|\Phi_Q|^4 + |\Phi_{-Q}|^4) + 2\beta|\Phi_Q|^2|\Phi_{-Q}|^2, \tag{21}$$

where β and β_ϱ are positive. Next rescaling the parameters and rearranging the terms in the free energy Eq. (21), we get

$$F_0[\Phi_Q, \Phi_{-Q}] = \alpha'(|\Phi_Q|^2 + |\Phi_{-Q}|^2) + \frac{1}{2}(|\Phi_Q|^2 + |\Phi_{-Q}|^2)^2 - \frac{\beta_\ell}{2}(|\Phi_Q|^2| - |\Phi_{-Q}|^2)^2, \tag{22}$$

where $\alpha' = \alpha_\phi/(\beta_\varrho + \beta)$ and $\beta_\ell = (\beta - \beta_\varrho)/(\beta_\varrho + \beta)$. β_ϱ is the self-interaction of both the fields Φ_Q and Φ_{-Q}, and β denotes the strength of the competition between the two fields. The rescaled parameter β_ℓ decides the nature of the PDW ground state. If $\beta < \beta_\varrho$ (i.e., $\beta_\ell < 0$), the free energy in Eq. (21) favors a coexisting ground state with ($\Phi_Q \neq 0, \Phi_{-Q} \neq 0$). On the other hand, $\beta > \beta_\varrho$ (i.e., $\beta_\ell > 0$) allows for a ground state with ($\Phi_Q \neq 0, \Phi_{-Q} = 0$) or ($\Phi_{-Q} \neq 0, \Phi_Q = 0$). These two states have a $\mathbb{Z}_2$ degeneracy due to $\mathcal{T}$-$\mathcal{P}$ symmetry, which is the same $\mathbb{Z}_2$ symmetry in the primary BDW order.

Now, we add the gradient terms in F_0 [Eq. (22)] to account for the thermal fluctuations of the composite PDW field in a 2D system, and we arrive at the following GL free energy:

$$F[\Phi_Q, \Phi_{-Q}] = \alpha'(|\Phi_Q|^2 + |\Phi_{-Q}|^2) + \frac{1}{2}(|\Phi_Q|^2 + |\Phi_{-Q}|^2)^2 - \frac{\beta_\ell}{2}(|\Phi_Q|^2 - |\Phi_{-Q}|^2)^2 + (|\nabla\Phi_Q|^2 + |\nabla\Phi_{-Q}|^2). \tag{23}$$

Incorporating the fluctuations in Φ_Q and Φ_{-Q} through Hubbard-Stratonovich transformations of the GL free energy Eq. (23) and using the saddle-point approximation, we study the possibility of the appearance of $\mathcal{T}$-$\mathcal{P}$ symmetry breaking without any requirement of $\mathcal{T}$-$\mathcal{P}$ symmetry breaking in the PDW ground state.

A. HS transformations and effective free energy

The partition function corresponding to the free energy Eq. (23) can be written as $Z[\Phi_Q, \Phi_{-Q}] \propto \int d\Phi_Q d\Phi_{-Q} \exp(-F[\Phi_Q, \Phi_{-Q}])$. We make a HS transformation of the partition function $Z[\Phi_Q, \Phi_{-Q}]$ to arrive at an effective partition function in terms of the HS fields. To this end, we introduce two conjugate HS fields as follows:

$$\varrho \equiv i(|\Phi_Q|^2 + |\Phi_{-Q}|^2),$$
$$\ell \equiv (|\Phi_Q|^2 - |\Phi_{-Q}|^2). \tag{24}$$

The HS field ℓ describes a "preemptive" MELC order. ϱ gives the Gaussian correction to susceptibility due to fluctuation. Now we make the following HS transformations in the partition function $Z[\Phi_Q, \Phi_{-Q}]$:

$$\exp\left[-\sum_{i=1}^{N}(|\Phi_{Q,i}|^2 + |\Phi_{-Q,i}|^2)^2/2N\right] = \sqrt{N/2\pi}\int d\varrho\, e^{\frac{-N\varrho^2}{2}} \exp\left[i\varrho\sum_{i=1}^{N}(|\Phi_{Q,i}|^2 + |\Phi_{-Q,i}|^2)\right],$$

$$\exp\left[\sum_{i=1}^{N}\beta_\ell(|\Phi_{Q,i}|^2 - |\Phi_{-Q,i}|^2)^2/2N\right] = \sqrt{N/2\pi}\int d\ell\, e^{\frac{-N\ell^2}{2\beta_\ell}} \exp\left[\ell\sum_{i=1}^{N}(|\Phi_{Q,i}|^2 - |\Phi_{-Q,i}|^2)\right],$$

where we have assumed that the PDW fields have N components, where $N \gg 1$. Next we take the limit $N \sim 1$, where the qualitative results for HS transformation are not expected to change [93,130]. Using the above HS transformations with $N = 1$ in the partition function $Z[\Phi_Q, \Phi_{-Q}]$, and integrating over Φ_Q and Φ_{-Q}, we obtain an effective partition function in terms of the HS fields ϱ and ℓ. The new effective partition can be written in terms of HS fields as

$$Z_{\text{eff}}[\varrho, \ell] \propto \int d\varrho\, d\ell \exp\left[-\frac{\varrho^2}{2} - \frac{\ell^2}{2\beta_\ell}\right] \exp\left[-\int \frac{d^2q}{4\pi^2}\ln[(\alpha' + q^2 - i\varrho)^2 - \ell^2]\right].$$

As the effective partition function can be written as $Z_{\text{eff}}[\varrho, \ell] \propto \int d\varrho\, d\ell \exp(-F_{\text{eff}}[\varrho, \ell])$, the effective free energy $F_{\text{eff}}[\varrho, \ell]$ is given by

$$F_{\text{eff}}[\varrho, \ell] = \frac{\varrho^2}{2} + \frac{\ell^2}{2\beta_\ell} + \int \frac{d^2q}{4\pi^2}\ln[(\alpha' + q^2 - i\varrho)^2 - \ell^2]. \tag{25}$$

B. Saddle-point analysis of the effective free energy

We consider that the fluctuations in the preemptive MELC order ℓ around the saddle-point solutions are small. Therefore, we continue with the saddle-point approximation for the free energy in terms of the MELC order parameter and closely follow the theoretical framework in Refs. [93,129].

The saddle point solutions are obtained by minimizing the free energy $F_{\text{eff}}[\varrho, \ell]$ with respect to ϱ and ℓ. These give the following equations for ϱ and ℓ:

$$\frac{\partial F_{\text{eff}}}{\partial \varrho} = 0 \Rightarrow \varrho = 2i\int \frac{d^2q}{4\pi^2}\frac{(\alpha' + q^2 - i\varrho)}{(\alpha' + q^2 - i\varrho)^2 - \ell^2} \tag{26}$$

and,

$$\frac{\partial F_{\text{eff}}}{\partial \ell} = 0 \Rightarrow \ell = 2\beta_\ell\int \frac{d^2q}{4\pi^2}\frac{\ell}{(\alpha' + q^2 - i\varrho)^2 - \ell^2}. \tag{27}$$

After performing the integration in Eqs. (26) and (27), we get the following two coupled equations for r and ℓ:

$$r = \alpha' + \frac{1}{4\pi}[\ln(\Lambda^2 - \ell^2) - \ln(r^2 - \ell^2)],$$
$$\ell = \frac{\beta_\ell}{2\pi}\coth^{-1}\left(\frac{r}{\ell}\right), \tag{28}$$

where $r = \alpha' - i\varrho$ and Λ is the upper momentum cutoff. We note that the solution of Eq. (26) exists only for imaginary ϱ, hence we replace ϱ by $i\varrho_0$ where ϱ is real. So, $\varrho = 0$ cannot be a solution. But $\ell = 0$ is an allowed solution. Therefore, we consider the following two cases: $\ell = 0, \varrho \neq 0$ and $\ell \neq 0, \varrho \neq 0$.

1. Case: $\ell = 0, \varrho \neq 0$

For the case $\ell = 0$, $\varrho \neq 0$, the solution for r can be rewritten from Eq. (28) as

$$r = \alpha' + \frac{1}{2\pi}\ln\left(\frac{\Lambda}{r}\right).$$

To find the stability of the solution, we need to analyze the condition for $\frac{\partial^2 F_{\text{eff}}[\varrho,\ell]}{\partial\varrho^2}|_{\varrho=i\varrho_0,\ell=0}$ and $\frac{\partial^2 F_{\text{eff}}[\varrho,\ell]}{\partial\ell^2}|_{\varrho=i\varrho_0,\ell=0}$ to be positive. We get the second derivatives to be as follows:

$$\left.\frac{\partial^2 F_{\text{eff}}[\varrho,\ell]}{\partial\varrho^2}\right|_{\ell=0} = 1 + 2i\int \frac{d^2q}{4\pi^2}\frac{-i}{(\alpha' + q^2 - i\varrho)^2} \tag{29}$$

and

$$\frac{\partial^2 F_{\text{eff}}[\varrho,\ell]}{\partial\ell^2} = \frac{1}{\beta_\ell} - 2\int\frac{d^2q}{4\pi^2}\left[\frac{1}{(\alpha' + q^2 - i\varrho)^2 - \ell^2} - \frac{2\ell^2}{[(\alpha' + q^2 - i\varrho)^2 - \ell^2]^2}\right]. \tag{30}$$

Next plugging $\varrho = i\varrho_0$ in Eq. (29) and performing the integration gives $\frac{\partial^2 F_{\text{eff}}[\varrho,\ell]}{\partial\varrho^2}|_{\varrho=i\varrho_0,\ell=0} = (1 + \frac{1}{2\pi r})$. Here, we used $r = \alpha' + \varrho_0$. The sign of r is always positive unless the PDW fields become ordered. Hence the value of $(1 + \frac{1}{2\pi r})$ is always positive. Again, performing the integration and plugging in the limits $\varrho = i\varrho_0$ and $\ell = 0$ in Eq. (30), we get $\frac{\partial^2 F_{\text{eff}}[\varrho,\ell]}{\partial\ell^2}|_{\varrho=i\varrho_0,\ell=0} = \frac{1}{\beta_\ell}(1 - \frac{\beta_\ell}{2\pi r})$. Now to hold $\frac{\partial^2 F_{\text{eff}}[\varrho,\ell]}{\partial\ell^2}|_{\varrho=i\varrho_0,\ell=0} > 0$, we need $(1 - \frac{\beta_\ell}{2\pi r}) > 0$ or $r > \frac{\beta_\ell}{2\pi}$. This condition, along with Eq. (28) for r, yields

$$\alpha' \geqslant \frac{\beta_\ell}{2\pi} - \frac{1}{2\pi}\ln\left(\frac{2\pi\Lambda}{\beta_\ell}\right).$$

This stability condition for r put a constraint on the mass term α' as

$$\alpha' \geqslant \alpha'_0, \tag{31}$$

with

$$\alpha'_0 = \frac{\beta_\ell}{2\pi} - \frac{1}{2\pi}\ln\left(\frac{2\pi\Lambda}{\beta_\ell}\right). \tag{32}$$

2. Case: $\ell \neq 0, \varrho \neq 0$

Here we analyze the state in which $\varrho \neq 0$ and $\ell \neq 0$, i.e., a state with preemptive MELC order. Eliminating r from Eq. (28), we arrive at the following equation for ℓ':

$$\frac{\beta_\ell}{2\pi}\ell'\coth\ell' - \frac{1}{2\pi}\ln\left(\frac{2\pi\Lambda}{\beta_\ell}\right) + \frac{1}{2\pi}\ln\left(\frac{\ell'}{\sinh\ell'}\right) = \alpha', \tag{33}$$

where

$$\ell' = \frac{2\pi\ell}{\beta_\ell}. \tag{34}$$

Substituting α'_0 from Eq. (32) in Eq. (33) and rearranging we get

$$1 - \frac{\ell'}{\tanh\ell'} + \frac{1}{\beta_\ell}\ln\left(\frac{\sinh\ell'}{\ell'}\right) = \frac{2\pi}{\beta_\ell}(\alpha'_0 - \alpha'). \tag{35}$$

The above equation gives the solution for ℓ'. We define the left hand side (LHS) of Eq. (35) as $g(\ell')$, i.e.,

$$g(\ell') = 1 - \frac{\ell'}{\tanh\ell'} + \frac{1}{\beta_\ell}\ln\left(\frac{\sinh\ell'}{\ell'}\right). \tag{36}$$

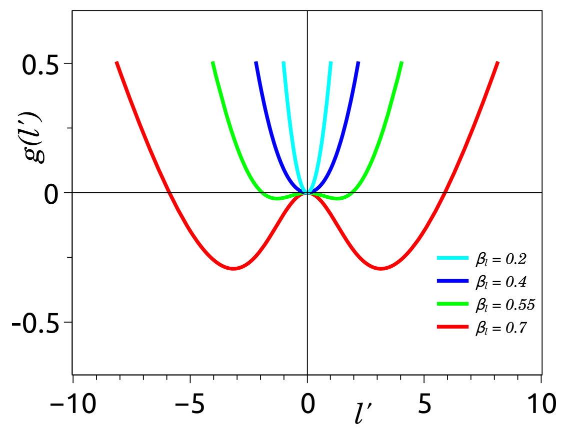

FIG. 4. Plots of $g(\ell')$ [defined in Eq. (36)] representing the LHS of Eq. (35), which gives the solution for the rescaled MELC order ℓ' [defined in Eq. (34)] for four different values of β_ℓ. In the range $0 < \beta_\ell < 0.5$, $g(\ell')$ shows only one minimum at $\ell' = 0$. On the other hand, in the range $0 < \beta_\ell < 0.5$, $g(\ell')$ acquires two minima for $\ell' \neq 0$, symmetric about $\ell' = 0$.

We plot $g(\ell')$ in Fig. 4 for different values of β_l. We notice that for $\ell' > 0$ and for $\beta_\ell < 0.5$, the function $f(\ell')$ is monotonically increasing, whereas for $1 > \beta_\ell > 0.5$, the function is not monotonically increasing. These are also true for $\ell' < 0$. We will show that the MELC order ℓ' can appear through two types of phase transitions depending on the parameter regime $0.5 > \beta_\ell > 0$ and $1 > \beta_\ell > 0.5$.

Second-order phase transition $(0.5 > \beta_\ell > 0)$. First we discuss the case $0.5 > \beta_\ell > 0$. The right hand side (RHS) of Eq. (35) can be rewritten as $\frac{2\pi}{\beta_\ell}\alpha'_0(1 - \alpha'/\alpha'_0)$, where α'_0 is also a function of β_ℓ and we consider $\alpha'_0 > 0$. Hence Eq. (35) becomes [using Eq. (36)]

$$g(\ell') = \frac{2\pi\alpha'_0}{\beta_\ell}(1 - \alpha'/\alpha'_0). \tag{37}$$

The plot in Fig. 5(a) represents a graphical representation of both sides of Eq. (37) for $\beta_\ell = 0.2$ and three different values of α'/α'_0. We notice that for $\alpha' < \alpha'_0$, the equation sustains

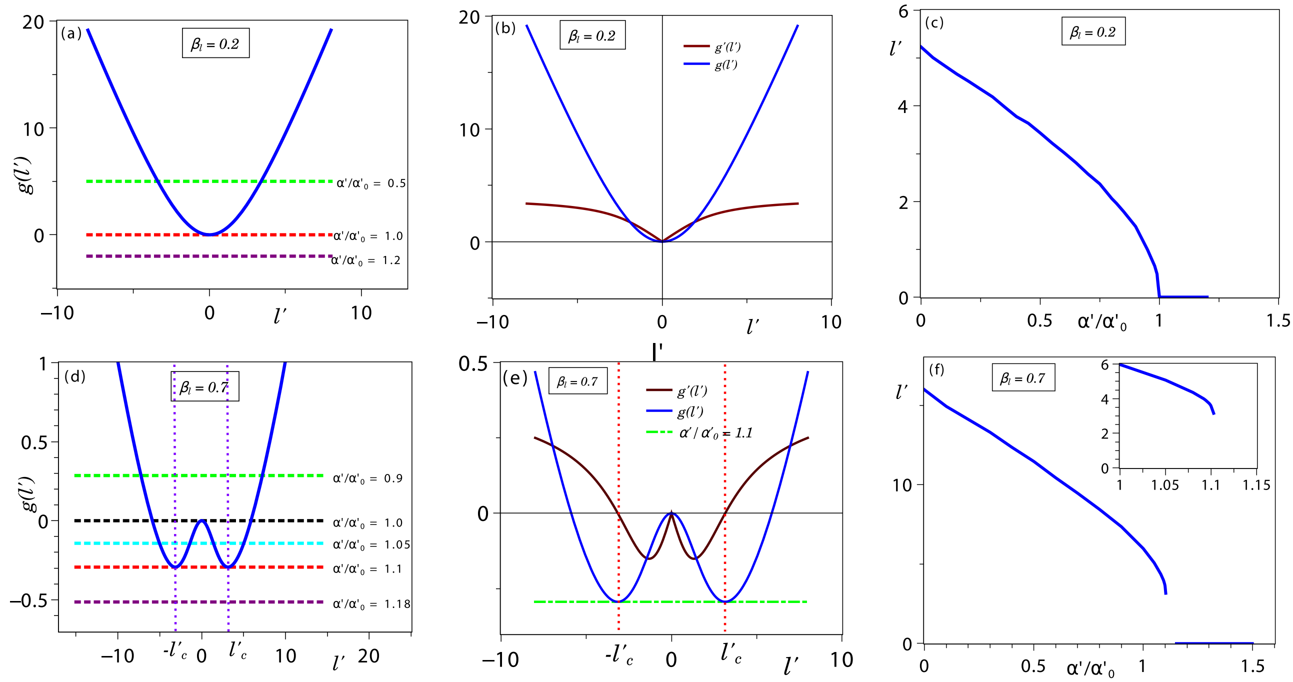

FIG. 5. Graphical analysis illustrating the nature of phase transitions of the preemptive MELC order. In (a) and (d), the LHS and RHS of the Eq. (37) is shown as solid and dashed lines, respectively. Intersections of the solid and dashed lines give the solutions of ℓ', where ℓ' is the rescaled MELC order as given in Eq. (34). The stability of the solutions is analyzed by looking at $g'(\ell')$ along with $g(\ell')$ as shown in (b) and (e). The allowed stable solutions of ℓ' are plotted in (c) and (f). The case of the second-order phase transition is shown in (a)–(c) with a choice $\beta_\ell = 0.2$. ℓ' continuously goes to zero at $\alpha'/\alpha'_0 = 1$ [the corresponding temperature is defined as T_0 in the Eq. (40)]. With the parametrization of α' in Eq. (39), $\alpha' = 0$ corresponds to $T = T_{\rm PDW}$, the mean-field transition temperature of the PDW field. The appearance of ℓ' at T_0 ($> T_{\rm PDW}$) shows that ℓ' is a preemptive order. The case of the first-order phase transition is shown in (d)–(f) with a representative $\beta_\ell = 0.7$. In contrast to the second-order case, in this case, solutions of ℓ' also exist for $\alpha'/\alpha'_0 > 1$. Although there exists a parameter regime in which there are four ℓ' values, a closer investigation at $g'(\ell')$ in (e) shows that the solutions in the range $-\ell'_c < \ell' < \ell'_c$ are not stable, hence they are not allowed. This creates a discontinuity in the allowed values of ℓ'. For the parameters considered in this plot, the discontinuous jump in ℓ' occurs at a value $\alpha'/\alpha'_0 = 1.1 > 1$ (the corresponding temperature is T'_0 and is also greater than $T_{\rm PDW}$). In all the plots, we have taken $\pi\alpha'_0 = 1$ for simplicity.

nonzero values for ℓ', while for $\alpha' = \alpha'_0$, ℓ' becomes zero, and for $\alpha' > \alpha'_0$, Eq. (37) has no solution. So, the order ℓ' appears first at $\alpha' = \alpha'_0$ and then increases as α'/α'_0 gets smaller. Whether the state with the values of ℓ', obtained from solution of Eq. (37), is stable or not can be seen by analyzing the second derivative of the effective free energy. The corresponding condition is $g'(\ell')|_{\ell'=\ell_0,-\ell_0} = \frac{\partial g(\ell')}{\partial \ell'}|_{\ell'=\ell_0,-\ell_0} > 0$, where ℓ_0 is a solution of Eq. (37). To analyze this condition, we determine $g'(\ell')|_{\ell'=\ell_0}$ and $g'(\ell')|_{\ell'=-\ell_0}$, which are given by the following equations:

$$g'(\ell')|_{\ell'=\ell_0} = \frac{1}{\beta_\ell}\left[\frac{1}{\tanh \ell_0} - \frac{1}{\ell_0}\right] - \left[\frac{1}{\tanh \ell_0} - \frac{\ell_0}{\sinh^2 \ell_0}\right],$$
$$g'(\ell')|_{\ell'=-\ell_0} = \frac{1}{\beta_\ell}\left[\frac{-1}{\tanh \ell_0} + \frac{1}{\ell_0}\right] - \left[\frac{-1}{\tanh \ell_0} + \frac{\ell_0}{\sinh^2 \ell_0}\right]. \tag{38}$$

$g'(\ell')$ and $g(\ell')$ for $\beta_\ell = 0.2$ are plotted in Fig. 5(b). We observe that in this case, $g'(\ell') > 0$ for all ℓ'. Hence all the solutions of ℓ' from Eq. (37) are allowed and correspond to the minima of the effective free energy.

The allowed values of ℓ' are plotted as a function of α'/α'_0 for $\beta_\ell = 0.2$ in Fig. 5(c). We notice that value of ℓ' continuously decreases to zero as α'/α'_0 approaches 1. This indicates a second-order phase transition in the MELC order ℓ'.

First-order phase transition ($1 > \beta_\ell > 0.5$). Here we discuss the case in which $1 > \beta_\ell > 0.5$. Again, we vary α'/α'_0 to find the solution of Eq. (37). We plot the LHS and RHS of Eq. (37) for $\beta_\ell = 0.7$ in Fig. 5(d). We observe that in this case, as α'/α'_0 is increased from 0 to 1, the value of ℓ' is nonzero, and it decreases as in the case of $\beta_\ell < 0.5$. But Eq. (37) also has a solution for $\alpha'/\alpha'_0 > 1.0$, which is in striking contrast to the $\beta_\ell < 0.5$ case. We also notice that for $\alpha'/\alpha'_0 > 1.0$, Eq. (37) has two solutions. To analyze whether both solutions are stable, we plot $g'(\ell')$ and $g(\ell')$ in Fig. 5(e) for the case $\beta_\ell = 0.7$. We observe that for $\ell' > \ell'_c$, as indicated by the red dotted line, $g'(\ell') > 0$, whereas for $\ell' < \ell'_c$, $g'(\ell') < 0$. This implies that all the values of $\ell' > \ell'_c$ are stable and therefore correspond to minima of the free energy. Hence, for the case $1 > \beta_\ell > 0.5$, the allowed values of ℓ' remain finite from $\alpha'/\alpha'_0 = 0$ until a certain value of $\alpha'/\alpha'_0 (> 1)$, and then suddenly they jump to zero as beyond that particular α'/α'_0 there exists no solution to Eq. (37).

In Fig. 5(f), we plot the allowed values of ℓ' as a function of α'/α'_0. We notice the discontinuous jump in ℓ' at a certain value of $\alpha'/\alpha'_0 (>1)$. This discontinuous change in ℓ' suggests a first-order phase transition.

Temperature dependence of ℓ': Preemptive MELC order. To study the temperature dependence of ℓ', we parametrize α' as

$$\alpha' = M'(T - T_{\rm PDW}), \tag{39}$$

where M' is a positive constant. The parametrization of α' is chosen in such a way that there is a mean-field phase transition at temperature $T = T_{\rm PDW}$ to a composite PDW order, i.e., when $\alpha' = 0$. Therefore, α' corresponding to some arbitrary temperature T_0 can be written as

$$\alpha'|_{T=T_0} \equiv \alpha'_0 = M'(T_0 - T_{\rm PDW}). \tag{40}$$

This leads to

$$T_0 = T_{\rm PDW} + \frac{\alpha'_0}{M'}. \tag{41}$$

We note that $\alpha' > \alpha'_0$ corresponds to temperature $T > T_0$ and $\alpha' < \alpha'_0$ to temperature $T < T_0$. Since $\alpha'_0 > 0$, we observe that T_0 is always larger than $T_{\rm PDW}$, which is the condensation temperature for the PDW fields. The MELC order appears through a continuous second-order phase transition for $0.5 > \beta_\ell > 0$, at temperature T_0, which is higher than $T_{\rm PDW}$. This indicates that the order ℓ' preempts the PDW order, hence the MELC order appears as a preemptive order in our analysis. As noted in Eq. (39), α'/α'_0 is directly proportional to the temperature. Consequently, for the first-order phase transition for $1.0 > \beta_\ell > 0.5$, the MELC order appears at a temperature T'_0. T'_0 is even higher than the second-order transition temperature T_0 and certainly greater than $T_{\rm PDW}$ [see Eq. (41)]. Thus, the MELC order preempts $T_{\rm PDW}$ even in this case of a first-order phase transition. Within our theoretical framework, the PDW order is a composite order of SC and BDW. Hence it becomes long-range only when both the primary orders SC and BDW become long-range. This suggests that the MELC order also preempts the primary SC and BDW orders. It is important to note that $\mathcal{T}$-$\mathcal{P}$ symmetry breaking has been experimentally observed at the pseudogap temperature T^* in the underdoped cuprates. The temperature T_0 can also be T^*. However, to establish whether the temperature T_0 is equal to T^* is beyond the scope of this work.

For the case of second-order transition, we extract the temperature dependence of ℓ' by obtaining the solutions of ℓ' in Fig. 5(c) and using the temperature parametrization of α' in Eq. (39). In Fig. 6, we plot the temperature dependence of ℓ' for $\beta_\ell = 0.2$. Close to the transition, an analytical temperature dependence of ℓ' can be obtained. If we expand the LHS of Eq. (37) for small values of ℓ', we find that

$$\frac{\ell'^2}{6\beta_\ell} = \frac{2\pi\alpha'_0}{\beta_\ell}(1 - \alpha'/\alpha'_0). \tag{42}$$

This gives

$$\ell'^2 = 12\pi(\alpha'_0 - \alpha') \tag{43}$$

or using Eqs. (39) and (40),

$$\ell' \propto (T_0 - T)^{1/2}. \tag{44}$$

Since we have only obtained the solutions for ℓ' within a HS saddle-point analysis, the fluctuations in ℓ' are not captured in our formalism. Thus, the critical exponent obtained here behaves similar to a mean-field Ising-like transition. Fluctuations of ℓ' can be considered within an alternate method such as the renormalization-group approach. Such an analysis to obtain a non-mean-field-like exponent is not a part of this study.

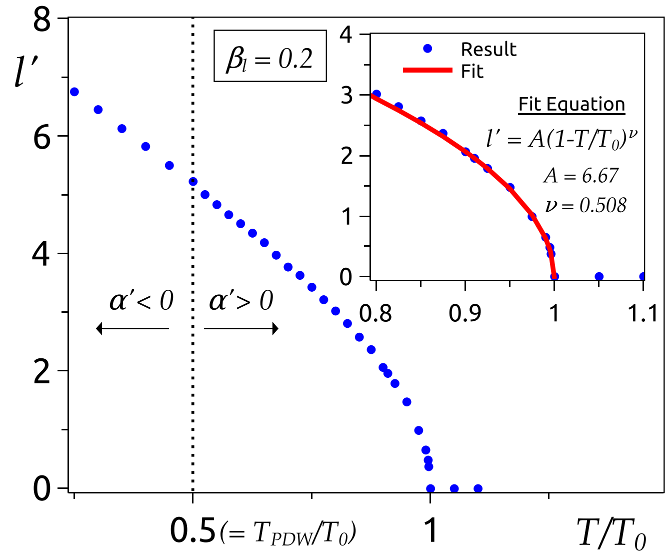

FIG. 6. A phase diagram of preemptive MELC order (ℓ') [defined in Eq. (34)] with scaled temperature T/T_0 for the case of second-order phase transition. Values of ℓ' are obtained from Fig. 5(c) and the temperature dependence is calculated using the parametrization of α' in Eq. (39). To plot this phase diagram, we have taken $T_0 = 1$ and $T_{\rm PDW}/T_0 = 0.5$ and $\beta_\ell = 0.2$. The plot shows ℓ' continuously changes across $T_{\rm PDW}$ where α' changes its sign. This indicates that the preemptive MELC order first emerges at temperature $T = T_0$ and can survive down to low temperatures. The inset shows a fit of the values of ℓ' in the main panel close to $T = T_0$ with a function $A(1 - T/T_0)^\nu$. The fitting parameter ν is found to be ≈ 0.5, close to the mean-field critical exponent in the Ising-like transition. A similar temperature dependence can be found directly from a low-order expansion of ℓ' in Eq. (35), which yields Eq. (44).

In the inset of Fig. 6, we show the temperature dependence of ℓ' close to the transition. Note that the points in this inset are obtained from the main panel and thus satisfy Eq. (35). As an independent check, we fit ℓ' for temperatures close to T_0 with a function $A(1 - T/T_0)^\nu$, where A and ν are fitting parameters. The value of ν obtained from the fit is consistent with the analytic expression of the temperature dependence in Eq. (44).

VI. DISCUSSIONS

A. Extension to tetragonal lattice systems

To construct the GL theory (see Secs. IV and V), we restrict ourselves to lattice systems having orthorhombic symmetry to simplify the analytic calculations. However, the GL framework presented in this paper can be extended to a larger order parameter manifold, relevant to lattice structure with higher symmetries.

To demonstrate, we construct the order parameter manifold and MELC order for tetragonal lattice systems with C_4

symmetry. For an orthorhombic system, the number of relevant hot-spots are two (numbered as 1 and 5 in Fig. 2) as described in Sec I. The order-parameter manifold is given in Eq. (4). We need seven unknown GL parameters to write down the corresponding free energy in Eq. (10) for this reduced order-parameter manifold. For a tetragonal crystal system, due to the presence of C_4 symmetry, the relevant hot-spots are 1, 3, 5, and 7. The order-parameter manifold in this case becomes

$$[\chi^1_{Q_x}, \chi^3_{Q_y}, \chi^5_{-Q_x}, \chi^7_{-Q_y}, \Delta]. \tag{45}$$

The GL free energy in this case can be written following a similar procedure to that in Sec. IV as

$$\begin{aligned}\mathcal{F} = {} & \alpha_d|\Delta|^2 + \alpha\big(|\chi^1_{Q_x}|^2 + |\chi^3_{Q_y}|^2 + |\chi^5_{-Q_x}|^2 + |\chi^7_{-Q_y}|^2\big)\\ & + \beta_1\big(|\chi^1_{Q_x}|^4 + |\chi^3_{Q_y}|^4 + |\chi^5_{-Q_x}|^4 + |\chi^7_{-Q_y}|^4\big)\\ & + \beta_d|\Delta|^4 + \beta_2\big(|\chi^1_{Q_x}|^2|\Delta|^2 + |\chi^5_{-Q_x}|^2|\Delta|^2 + |\chi^3_{Q_y}|^2|\Delta|^2\\ & + |\chi^7_{-Q_y}|^2|\Delta|^2\big) + \beta_3\big(|\chi^1_{Q_x}|^2|\chi^5_{-Q_x}|^2 + |\chi^3_{Q_y}|^2|\chi^7_{-Q_y}|^2\big)\\ & + \beta_5\big(|\chi^1_{Q_x}|^2|\chi^3_{Q_y}|^2 + |\chi^5_{-Q_x}|^2|\chi^7_{-Q_y}|^2 + |\chi^3_{Q_y}|^2|\chi^5_{-Q_x}|^2\\ & + |\chi^1_{Q_x}|^2|\chi^7_{-Q_y}|^2\big).\end{aligned} \tag{46}$$

Here also, we notice that the free energy Eq. (46) remains invariant under all point group operations of tetragonal system, parity, time-reversal, translation, and gauge symmetry transformations. While writing the free energy in Eq. (46), we have not shown the terms that give rise to purely imaginary BDW ground states for simplicity. An enhanced number of BDW order parameters in the manifold [Eq. (45)] for the tetragonal case gives an increased number of possible mean-field solutions compared to the orthorhombic case. Furthermore, the number of unknown GL parameters is also increased in Eq. (46). So, the analysis of even the various mean-field solutions of Eq. (46) becomes analytically cumbersome.

B. Possible relevance to experiments

In this section, we present possible outcomes of our analysis in connection to experimental observations in underdoped cuprates. Though our analysis of $\mathcal{T}$-$\mathcal{P}$ symmetry breaking is based on phenomenological motivations drawn from experiments in underdoped cuprates, here we focus only on qualitative relevance to experiments due to the simplistic nature of the crystal structure considered in this paper.

We demonstrated in Sec. V that the preemptive MELC order can appear through two types of phase transitions. First, it can appear through a continuous second-order phase transition at a temperature higher than T_{PDW}. Importantly, the phase transition temperatures can also be equal to T^*. The signatures of the appearance of IUC magnetism breaking $\mathcal{T}$-$\mathcal{P}$ symmetry at T^* through a second-order transition have been reported in some spin-polarized neutron diffraction experiments [131–134]. Second, the MELC order can also appear through a discontinuous first-order phase transition at a temperature that is again higher than T_{PDW} and even higher than the second-order phase transition temperature. To the best of our knowledge, there has been no experiment indicating a first-order phase transition to a $\mathcal{T}$-$\mathcal{P}$ broken state.

Spin-polarized neutron scattering experiments measure the magnetic neutron intensity to describe the $\vec{Q} = 0$ magnetism in the PG phase of cuprates. The observations [18,20,131] allowed the authors to deduce a critical exponent corresponding to the temperature dependence of the magnetic scattering intensity, although varying in a wide range of values from 0.25 to 0.5. Within our framework, in the case of the second-order phase transition in Sec. V B, the temperature dependence of the preemptive MELC order ℓ' close to the phase transition is obtained as $\ell' \sim (T_0 - T)^{1/2}$ [Eq. (44)]. This yields a critical exponent of ℓ' to be 0.5. But it must be noted that a quantitative comparison of the exponents would require more accuracy in experimental results and also the consideration of fluctuations in ℓ' using other theoretical tools like the renormalization-group treatment.

For $T < T_{\text{PDW}}$, the GL parameter $\alpha' < 0$ as seen from Eq. (39). Remarkably even for $\alpha' < 0$, Eq. (37) has allowed solutions for both the cases $0.5 > \beta_\ell > 0$ and $1 > \beta_\ell > 0.5$. Therefore, the MELC order ℓ' has a nonzero value for $\alpha' < 0$ and continuously changes when α' becomes greater than zero. This shows that the preemptive MELC order persists below the temperature T_{PDW}. Figure 6 shows the existence of MELC order at low temperatures for the second-order phase transition. This is also true for the first-order phase transition, although no signature of MELC order has been reported at low temperatures in the superconducting state for technical issues so far. This will motivate further experiments investigating $\mathcal{T}$-$\mathcal{P}$ symmetry breaking at low temperatures in the superconducting state.

It is also interesting to discuss the effects of the impurities on the MELC state. Strong substitutional impurities like Zn destroys the superconducting order parameter locally. The local MELC order parameter is given as $\ell \propto |\Phi_i|^2 \propto |\Delta_{ij}|^2|\chi_{ij}|^2$, where Δ_{ij} and χ_{ij} are superconducting and BDW order parameters, respectively. The MELC order parameter is thus suppressed close to the impurities. As a result, the MELC order parameter is reduced with an increase in Zn concentration. This might explain the reduction in the intensity of the IUC signal in polarized neutron diffraction measurement with Zn doping [135].

VII. CONCLUSION

Considering SC and BDW as primary orders, in this paper we explored possibility of $\mathcal{T}$-$\mathcal{P}$ symmetry breaking in the PG state of underdoped cuprates. We found that the thermal fluctuations of SC and BDW fields and consequently the fluctuations in the composite PDW fields result in a $\mathcal{T}$-$\mathcal{P}$ symmetry-breaking preemptive MELC ground state.

As a first step, within the GL mean-field theory of competing primary BDW and SC orders, we explored the existence of the MELC order in various parameter regimes and presented the conditions for the stability of the mean-field MELC state. We showed that the mean-field MELC order can emerge only in a phase where SC and BDW coexist. This mean-field MELC order is restricted to a situation in which the BDW ground state itself breaks $\mathcal{T}$-$\mathcal{P}$. However, there is no experimental evidence of such a BDW ground state.

We then considered the fluctuations of the SC and BDW fields in the free energy. We notice that fluctuations in SC and BDW fields lead to fluctuations in composite PDW fields. Treating the thermal fluctuations of the PDW fields in a Hubbard-Stratonovich approach, we then showed that a nontrivial MELC order preempts at a temperature above $T_{\rm PDW}$, the mean-field PDW transition temperature. The analysis showed that the $\mathcal{T}$-$\mathcal{P}$ symmetry is spontaneously broken in the preemptive MELC state even though the PDW ground states preserve the symmetry. This also suggests that the BDW ground state does not need to break $\mathcal{T}$-$\mathcal{P}$ symmetry. We described that, depending on parameter regime, the preemptive MELC order can emerge through both second- and first-order phase transition.

ACKNOWLEDGMENTS

We thank Y. Sidis for valuable discussions. This work has received financial support from the ERC, under Grant Agreement AdG-694651-CHAMPAGNE.

APPENDIX: DETAILS OF MEAN-FIELD GL THEORY

In this Appendix, we analytically calculate the mean-field solutions of the free energy density Eq. (10) for competing BDW and SC. The possible ground states for the primary order parameters (χ_Q, χ_{-Q}, Δ) manifold are shown in Table II. For each ground state, we calculate the mean-field free energy, which enables us to find the stability criteria of the ground state sustaining a nonzero MELC order.

1. Ground state $(a, 0, b)$

The free energy density functional for this state can be obtained from Eq. (10) and is given by

$$F = \alpha_d|\Delta|^2 + \alpha|\chi_Q|^2 + \frac{\beta_1}{2}|\chi_Q|^4 + \frac{\beta_d}{2}|\Delta|^4 + \beta_2|\chi_Q|^2|\Delta|^2. \tag{A1}$$

Minimization of the free energy with respect to χ_Q and Δ leads to the following two mean-field equations:

$$\alpha + \beta_1|\chi_Q|^2 + \beta_2|\Delta|^2 = 0 \tag{A2}$$

and

$$\alpha_d + \beta_d|\Delta|^2 + \beta_2|\chi_Q|^2 = 0. \tag{A3}$$

The above two equations give the mean-field values of χ_Q and Δ to be

$$\chi_Q^2 = \frac{\beta_2\alpha_d - \alpha\beta_d}{\beta_1\beta_d - \beta_2^2},$$
$$\Delta^2 = \frac{\alpha\beta_2 - \alpha_d\beta_1}{\beta_1\beta_d - \beta_2^2}. \tag{A4}$$

Substituting the above solution in the mean-field free energy, we get

$$F(a, 0, b) = \frac{[2\alpha\alpha_d\beta_2 - \alpha_d^2\beta_1 - \alpha^2\beta_d]}{2[\beta_1\beta_d - \beta_2^2]}. \tag{A5}$$

2. Ground state (a, a, b)

The free energy density functional in this case can be written from Eq. (10) as

$$F = \alpha_d|\Delta|^2 + 2\alpha|\chi_Q|^2 + \beta_1|\chi_Q|^4 + \frac{\beta_d}{2}|\Delta|^4 + 2\beta_2|\chi_Q|^2|\Delta|^2 + \beta_3|\chi_Q|^4 + 2\beta_4|\chi_Q|^2|\Delta|^2. \tag{A6}$$

Minimizing the free energy Eq. (A6) with respect to χ_Q and Δ gives

$$\alpha + \chi_Q^2(\beta_1 + \beta_3) + \Delta^2(\beta_2 + \beta_4) = 0 \tag{A7}$$

and

$$\alpha_d + 2(\beta_2 + \beta_4)\chi_Q^2 + \beta_d\Delta^2 = 0. \tag{A8}$$

The above two equations give the mean-field solution as

$$\chi_Q^2 = \frac{\alpha_d(\beta_2 + \beta_4) - \alpha\beta_d}{\beta_d(\beta_1 + \beta_3) - 2(\beta_2 + \beta_4)^2},$$
$$\Delta^2 = \frac{2\alpha(\beta_2 + \beta_4) - \alpha_d(\beta_1 + \beta_3)}{\beta_d(\beta_1 + \beta_3) - 2(\beta_2 + \beta_4)^2}. \tag{A9}$$

The mean-field free energy corresponding to this solution is

$$F(a, a, b) = \frac{4\alpha\alpha_d(\beta_2 + \beta_4) - \alpha_d^2(\beta_1 + \beta_3) - 2\alpha^2\beta_d}{2\beta_d(\beta_1 + \beta_3) - 4(\beta_2 + \beta_4)^2}. \tag{A10}$$

3. Ground state $(a, 0, 0)$

The free energy density Eq. (10) in this state can be written as

$$F = \alpha|\chi_Q|^2 + \frac{\beta_1}{2}|\chi_Q|^4. \tag{A11}$$

Minimizing the above free energy with respect to χ_Q gives

$$\chi_Q^2 = \frac{-\alpha}{\beta_1}. \tag{A12}$$

The mean-field free energy corresponding to this state is given by

$$F(a, 0, 0) = \frac{-\alpha^2}{2\beta_1}. \tag{A13}$$

4. Ground state $(0, 0, b)$

The free energy Eq. (10) in this state is given by

$$F = \alpha_d|\Delta|^2 + \frac{\beta_d}{2}|\Delta|^4. \tag{A14}$$

Minimizing the above free energy with respect to Δ gives

$$\Delta^2 = \frac{-\alpha_d}{\beta_d}. \tag{A15}$$

The corresponding mean-field free energy for the ground state is

$$F(0,0,b) = \frac{-\alpha_d^2}{2\beta_d}. \tag{A16}$$

5. Ground state $(a, a, 0)$

Finally we consider the case in which only BDW is nonzero and no SC is present.

The free energy in Eq. (10) becomes

$$F = 2\alpha|\chi_Q|^2 + \beta_1|\chi_Q|^4 + \beta_3|\chi_Q|^4. \tag{A17}$$

Minimizing the free energy with respect to χ_Q gives

$$\chi_Q^2 = \frac{-\alpha}{(\beta_1+\beta_3)}. \tag{A18}$$

The mean-field free energy for this ground state is

$$F(a,a,0) = \frac{-\alpha^2}{(\beta_1+\beta_3)}. \tag{A19}$$

[1] H. Alloul, T. Ohno, and P. Mendels, Phys. Rev. Lett. **63**, 1700 (1989).
[2] W. W. Warren, R. E. Walstedt, G. F. Brennert, R. J. Cava, R. Tycko, R. F. Bell, and G. Dabbagh, Phys. Rev. Lett. **62**, 1193 (1989).
[3] R. E. Walstedt, W. W. Warren, R. F. Bell, R. J. Cava, G. P. Espinosa, L. F. Schneemeyer, and J. V. Waszczak, Phys. Rev. B **41**, 9574 (1990).
[4] H. Alloul, P. Mendels, H. Casalta, J. F. Marucco, and J. Arabski, Phys. Rev. Lett. **67**, 3140 (1991).
[5] R. E. Walstedt, R. F. Bell, and D. B. Mitzi, Phys. Rev. B **44**, 7760 (1991).
[6] C. Berthier, M. Julien, M. Horvatić, and Y. Berthier, J. Phys. I **6**, 2205 (1996).
[7] D. S. Marshall, D. S. Dessau, A. G. Loeser, C.-H. Park, A. Y. Matsuura, J. N. Eckstein, I. Bozovic, P. Fournier, A. Kapitulnik, W. E. Spicer, and Z.-X. Shen, Phys. Rev. Lett. **76**, 4841 (1996).
[8] J. M. Harris, P. J. White, Z.-X. Shen, H. Ikeda, R. Yoshizaki, H. Eisaki, S. Uchida, W. D. Si, J. W. Xiong, Z.-X. Zhao, and D. S. Dessau, Phys. Rev. Lett. **79**, 143 (1997).
[9] C. Renner, B. Revaz, J.-Y. Genoud, K. Kadowaki, and O. Fischer, Phys. Rev. Lett. **80**, 149 (1998).
[10] A. Ino, T. Mizokawa, K. Kobayashi, A. Fujimori, T. Sasagawa, T. Kimura, K. Kishio, K. Tamasaku, H. Eisaki, and S. Uchida, Phys. Rev. Lett. **81**, 2124 (1998).
[11] J. Tallon and J. Loram, Physica C **349**, 53 (2001).
[12] F. Ronning, T. Sasagawa, Y. Kohsaka, K. M. Shen, A. Damascelli, C. Kim, T. Yoshida, N. P. Armitage, D. H. Lu, D. L. Feng, L. L. Miller, H. Takagi, and Z.-X. Shen, Phys. Rev. B **67**, 165101 (2003).
[13] K. McElroy, G.-H. Gweon, S. Y. Zhou, J. Graf, S. Uchida, H. Eisaki, H. Takagi, T. Sasagawa, D.-H. Lee, and A. Lanzara, Phys. Rev. Lett. **96**, 067005 (2006).
[14] A. Shekhter, B. J. Ramshaw, R. Liang, W. N. Hardy, D. A. Bonn, F. F. Balakirev, R. D. McDonald, J. B. Betts, S. C. Riggs, and A. Migliori, Nature (London) **498**, 75 (2013).
[15] B. Ramshaw, S. Sebastian, R. McDonald, J. Day, B. Tan, Z. Zhu, J. Betts, R. Liang, D. Bonn, W. Hardy *et al.*, Science **348**, 317 (2015).
[16] A. Kaminski, S. Rosenkranz, H. Fretwell, J. Campuzano, Z. Li, H. Raffy, W. Cullen, H. You, C. Olson, C. Varma *et al.*, Nature (London) **416**, 610 (2002).
[17] B. Fauqué, Y. Sidis, V. Hinkov, S. Pailhès, C. T. Lin, X. Chaud, and P. Bourges, Phys. Rev. Lett. **96**, 197001 (2006).
[18] H. A. Mook, Y. Sidis, B. Fauqué, V. Balédent, and P. Bourges, Phys. Rev. B **78**, 020506(R) (2008).
[19] Y. Li, V. Balédent, N. Barišić, Y. Cho, B. Fauque, Y. Sidis, G. Yu, X. Zhao, P. Bourges, and M. Greven, Nature (London) **455**, 372 (2008).
[20] Y. Li, V. Balédent, N. Barišić, Y. C. Cho, Y. Sidis, G. Yu, X. Zhao, P. Bourges, and M. Greven, Phys. Rev. B **84**, 224508 (2011).
[21] S. De Almeida-Didry, Y. Sidis, V. Balédent, F. Giovannelli, I. Monot-Laffez, and P. Bourges, Phys. Rev. B **86**, 020504(R) (2012).
[22] V. Balédent, B. Fauqué, Y. Sidis, N. B. Christensen, S. Pailhès, K. Conder, E. Pomjakushina, J. Mesot, and P. Bourges, Phys. Rev. Lett. **105**, 027004 (2010).
[23] L. Zhao, C. A. Belvin, R. Liang, D. A. Bonn, W. N. Hardy, N. P. Armitage, and D. Hsieh, Nat. Phys. **13**, 250 (2016).
[24] R.-H. He, M. Hashimoto, H. Karapetyan, J. D. Koralek, J. P. Hinton, J. P. Testaud, V. Nathan, Y. Yoshida, H. Yao, K. Tanaka, W. Meevasana, R. G. Moore, D. H. Lu, S.-K. Mo, M. Ishikado, H. Eisaki, Z. Hussain, T. P. Devereaux, S. A. Kivelson, J. Orenstein, A. Kapitulnik, and Z.-X. Shen, Science **331**, 1579 (2011).
[25] A. Kapitulnik, J. Xia, E. Schemm, and A. Palevski, New J. Phys. **11**, 055060 (2009).
[26] H. Karapetyan, M. Hücker, G. D. Gu, J. M. Tranquada, M. M. Fejer, J. Xia, and A. Kapitulnik, Phys. Rev. Lett. **109**, 147001 (2012).
[27] V. M. Yakovenko, Physica B **460**, 159 (2015).
[28] H. Karapetyan, J. Xia, M. Hücker, G. D. Gu, J. M. Tranquada, M. M. Fejer, and A. Kapitulnik, Phys. Rev. Lett. **112**, 047003 (2014).
[29] V. Aji, Y. He, and C. M. Varma, Phys. Rev. B **87**, 174518 (2013).
[30] S. S. Pershoguba, K. Kechedzhi, and V. M. Yakovenko, Phys. Rev. Lett. **111**, 047005 (2013).
[31] M. J. Lawler, K. Fujita, J. Lee, A. Schmidt, Y. Kohsaka, C. K. Kim, H. Eisaki, S. Uchida, J. C. Davis, J. P. Sethna, and E.-A. Kim, Nature (London) **466**, 347 (2010).
[32] Y. Kohsaka, C. Taylor, K. Fujita, A. Schmidt, C. Lupien, T. Hanaguri, M. Azuma, M. Takano, H. Eisaki, H. Takagi, S. Uchida, and J. C. Davis, Science **315**, 1380 (2007).
[33] R. Daou, J. Chang, D. Leboeuf, O. Cyr-Choinière, F. Laliberté, N. Doiron-Leyraud, B. J. Ramshaw, R. Liang, D. A. Bonn, W. N. Hardy, and L. Taillefer, Nature (London) **463**, 519 (2010).

[34] Y. Sato, S. Kasahara, H. Murayama, Y. Kasahara, E. G. Moon, T. Nishizaki, T. Loew, J. Porras, B. Keimer, T. Shibauchi, and Y. Matsuda, Nat. Phys. **13**, 1074 (2017).
[35] L. Mangin-Thro, Y. Li, Y. Sidis, and P. Bourges, Phys. Rev. Lett. **118**, 097003 (2017).
[36] C. M. Varma, Phys. Rev. B **55**, 14554 (1997).
[37] C. M. Varma, Phys. Rev. Lett. **83**, 3538 (1999).
[38] M. E. Simon and C. M. Varma, Phys. Rev. Lett. **89**, 247003 (2002).
[39] C. M. Varma, Phys. Rev. B **73**, 155113 (2006).
[40] M. E. Simon and C. M. Varma, Phys. Rev. B **67**, 054511 (2003).
[41] P. Chudzinski, M. Gabay, and T. Giamarchi, Phys. Rev. B **78**, 075124 (2008).
[42] M. H. Fischer and E.-A. Kim, Phys. Rev. B **84**, 144502 (2011).
[43] S. Bulut, A. P. Kampf, and W. A. Atkinson, Phys. Rev. B **92**, 195140 (2015).
[44] V. S. de Carvalho, C. Pépin, and H. Freire, Phys. Rev. B **93**, 115144 (2016).
[45] W. A. Atkinson, A. P. Kampf, and S. Bulut, Phys. Rev. B **93**, 134517 (2016).
[46] M. S. Scheurer and S. Sachdev, Phys. Rev. B **98**, 235126 (2018).
[47] M. Greiter and R. Thomale, Phys. Rev. Lett. **99**, 027005 (2007).
[48] R. Thomale and M. Greiter, Phys. Rev. B **77**, 094511 (2008).
[49] C. Weber, A. Läuchli, F. Mila, and T. Giamarchi, Phys. Rev. Lett. **102**, 017005 (2009).
[50] G. Ghiringhelli, M. Le Tacon, M. Minola, S. Blanco-Canosa, C. Mazzoli, N. B. Brookes, G. M. De Luca, A. Frano, D. G. Hawthorn, F. He, T. Loew, M. M. Sala, D. C. Peets, M. Salluzzo, E. Schierle, R. Sutarto, G. A. Sawatzky, E. Weschke, B. Keimer, and L. Braicovich, Science **337**, 821 (2012).
[51] J. Chang, E. Blackburn, A. T. Holmes, N. B. Christensen, J. Larsen, J. Mesot, R. Liang, D. A. Bonn, W. N. Hardy, A. Watenphul, M. v. Zimmermann, E. M. Forgan, and S. M. Hayden, Nat. Phys. **8**, 871 (2012).
[52] H.-H. Wu, M. Buchholz, C. Trabant, C. Chang, A. Komarek, F. Heigl, M. Zimmermann, M. Cwik, F. Nakamura, M. Braden *et al.*, Nat. Commun. **3**, 1023 (2012).
[53] A. J. Achkar, R. Sutarto, X. Mao, F. He, A. Frano, S. Blanco-Canosa, M. Le Tacon, G. Ghiringhelli, L. Braicovich, M. Minola, M. Moretti Sala, C. Mazzoli, R. Liang, D. A. Bonn, W. N. Hardy, B. Keimer, G. A. Sawatzky, and D. G. Hawthorn, Phys. Rev. Lett. **109**, 167001 (2012).
[54] E. Blackburn, J. Chang, M. Hücker, A. T. Holmes, N. B. Christensen, R. Liang, D. A. Bonn, W. N. Hardy, U. Rütt, O. Gutowski, M. v. Zimmermann, E. M. Forgan, and S. M. Hayden, Phys. Rev. Lett. **110**, 137004 (2013).
[55] E. Blackburn, J. Chang, A. H. Said, B. M. Leu, R. Liang, D. A. Bonn, W. N. Hardy, E. M. Forgan, and S. M. Hayden, Phys. Rev. B **88**, 054506 (2013).
[56] S. Blanco-Canosa, A. Frano, T. Loew, Y. Lu, J. Porras, G. Ghiringhelli, M. Minola, C. Mazzoli, L. Braicovich, E. Schierle, E. Weschke, M. Le Tacon, and B. Keimer, Phys. Rev. Lett. **110**, 187001 (2013).
[57] T. P. Croft, C. Lester, M. S. Senn, A. Bombardi, and S. M. Hayden, Phys. Rev. B **89**, 224513 (2014).
[58] E. H. da Silva Neto, P. Aynajian, A. Frano, R. Comin, E. Schierle, E. Weschke, A. Gyenis, J. Wen, J. Schneeloch, Z. Xu, S. Ono, G. Gu, M. Le Tacon, and A. Yazdani, Science **343**, 393 (2014).
[59] J. E. Hoffman, E. W. Hudson, K. M. Lang, V. Madhavan, H. Eisaki, S. Uchida, and J. C. Davis, Science **295**, 466 (2002).
[60] K. Matsuba, S. Yoshizawa, Y. Mochizuki, T. Mochiku, K. Hirata, and N. Nishida, J. Phys. Soc. Jpn. **76**, 063704 (2007).
[61] K. Fujita, C. K. Kim, I. Lee, J. Lee, M. Hamidian, I. A. Firmo, S. Mukhopadhyay, H. Eisaki, S. Uchida, M. J. Lawler, E. A. Kim, and J. C. Davis, Science **344**, 612 (2014).
[62] T. Machida, Y. Kohsaka, K. Matsuoka, K. Iwaya, T. Hanaguri, and T. Tamegai, Nat. Commun. **7**, 11747 (2016).
[63] M. H. Hamidian, S. D. Edkins, C. K. Kim, J. C. Davis, A. P. Mackenzie, H. Eisaki, S. Uchida, M. J. Lawler, E.-A. Kim, S. Sachdev, and K. Fujita, Nat. Phys. **12**, 150 (2015).
[64] R. Comin, R. Sutarto, F. He, E. H. da Silva Neto, L. Chauviere, A. Frano, R. Liang, W. N. Hardy, D. A. Bonn, Y. Yoshida, H. Eisaki, A. J. Achkar, D. G. Hawthorn, B. Keimer, G. A. Sawatzky, and A. Damascelli, Nat. Mater. **14**, 796 (2015).
[65] A. J. Achkar, F. He, R. Sutarto, J. Geck, H. Zhang, Y.-J. Kim, and D. G. Hawthorn, Phys. Rev. Lett. **110**, 017001 (2013).
[66] T. Wu, H. Mayaffre, S. Krämer, M. Horvatic, C. Berthier, W. N. Hardy, R. Liang, D. A. Bonn, and M.-H. Julien, Nature (London) **477**, 191 (2011).
[67] T. Wu, H. Mayaffre, S. Krämer, M. Horvatić, C. Berthier, P. L. Kuhns, A. P. Reyes, R. Liang, W. N. Hardy, D. A. Bonn, and M.-H. Julien, Nat. Commun. **4**, 2113 (2013).
[68] J. Chang, E. Blackburn, O. Ivashko, A. T. Holmes, N. B. Christensen, M. Hücker, R. Liang, D. A. Bonn, W. N. Hardy, U. Rütt, M. V. Zimmermann, E. M. Forgan, and S. M. Hayden, Nat. Commun. **7**, 11494 (2016).
[69] S. Gerber, H. Jang, H. Nojiri, S. Matsuzawa, H. Yasumura, D. A. Bonn, R. Liang, W. N. Hardy, Z. Islam, A. Mehta, S. Song, M. Sikorski, D. Stefanescu, Y. Feng, S. A. Kivelson, T. P. Devereaux, Z.-X. Shen, C. C. Kao, W. S. Lee, D. Zhu, and J. S. Lee, Science **350**, 949 (2015).
[70] H. Jang, W.-S. Lee, H. Nojiri, S. Matsuzawa, H. Yasumura, L. Nie, A. V. Maharaj, S. Gerber, Y.-J. Liu, A. Mehta, D. A. Bonn, R. Liang, W. N. Hardy, C. A. Burns, Z. Islam, S. Song, J. Hastings, T. P. Devereaux, Z.-X. Shen, S. A. Kivelson, C.-C. Kao, D. Zhu, and J.-S. Lee, Proc. Natl. Acad. Sci. USA **113**, 14645 (2016).
[71] D. LeBoeuf, S. Kramer, W. N. Hardy, R. Liang, D. A. Bonn, and C. Proust, Nat. Phys. **9**, 79 (2013).
[72] F. Laliberté, M. Frachet, S. Benhabib, B. Borgnic, T. Loew, J. Porras, M. Le Tacon, B. Keimer, S. Wiedmann, C. Proust, and D. LeBoeuf, npj Quantum Mater. **3**, 11 (2018).
[73] T. Wu, H. Mayaffre, S. Krämer, M. Horvatić, C. Berthier, W. N. Hardy, R. Liang, D. A. Bonn, and M.-H. Julien, Nat. Commun. **6**, 6438 (2015).
[74] M. H. Hamidian, S. D. Edkins, S. H. Joo, A. Kostin, H. Eisaki, S. Uchida, M. J. Lawler, E.-A. Kim, A. P. Mackenzie, K. Fujita, J. Lee, and J. C. S. Davis, Nature (London) **532**, 343 (2016).
[75] A. Larkin and I. Ovchinnikov, Sov. Phys. JETP **20**, 762 (1965).
[76] P. Fulde and R. A. Ferrell, Phys. Rev. **135**, A550 (1964).

[77] D. F. Agterberg, J. C. Séamus Davis, S. D. Edkins, E. Fradkin, D. J. Van Harlingen, S. A. Kivelson, P. A. Lee, L. Radzihovsky, J. M. Tranquada, and Y. Wang, arXiv:1904.09687.
[78] S. D. Edkins, A. Kostin, K. Fujita, A. P. Mackenzie, H. Eisaki, S. Uchida, S. Sachdev, M. J. Lawler, E. A. Kim, J. C. Séamus Davis, and M. H. Hamidian, Science **364**, 976 (2019).
[79] P. A. Lee, N. Nagaosa, and X.-G. Wen, Rev. Mod. Phys. **78**, 17 (2006).
[80] V. J. Emery and S. A. Kivelson, Nature (London) **374**, 434 (1995).
[81] S. Banerjee, T. V. Ramakrishnan, and C. Dasgupta, Phys. Rev. B **83**, 024510 (2011).
[82] M. R. Norman, M. Randeria, H. Ding, and J. C. Campuzano, Phys. Rev. B **57**, R11093 (1998).
[83] C.-C. Chien, Y. He, Q. Chen, and K. Levin, Phys. Rev. B **79**, 214527 (2009).
[84] R. Boyack, Q. Chen, A. A. Varlamov, and K. Levin, Phys. Rev. B **97**, 064503 (2018).
[85] E. Fradkin, S. A. Kivelson, and J. M. Tranquada, Rev. Mod. Phys. **87**, 457 (2015).
[86] B. Keimer, S. A. Kivelson, M. R. Norman, S. Uchida, and J. Zaanen, Nature (London) **518**, 179 (2015).
[87] S. Chatterjee, S. Sachdev, and A. Eberlein, Phys. Rev. B **96**, 075103 (2017).
[88] S. Sachdev, H. D. Scammell, M. S. Scheurer, and G. Tarnopolsky, Phys. Rev. B **99**, 054516 (2019).
[89] X.-G. Wen and P. A. Lee, Phys. Rev. Lett. **76**, 503 (1996).
[90] P. A. Lee, N. Nagaosa, T.-K. Ng, and X.-G. Wen, Phys. Rev. B **57**, 6003 (1998).
[91] K. B. Efetov, H. Meier, and C. Pépin, Nat. Phys. **9**, 442 (2013).
[92] M. A. Metlitski and S. Sachdev, New J. Phys. **12**, 105007 (2010).
[93] Y. Wang and A. Chubukov, Phys. Rev. B **90**, 035149 (2014).
[94] Y. Wang, S. D. Edkins, M. H. Hamidian, J. C. Séamus Davis, E. Fradkin, and S. A. Kivelson, Phys. Rev. B **97**, 174510 (2018).
[95] Z. Dai, Y.-H. Zhang, T. Senthil, and P. A. Lee, Phys. Rev. B **97**, 174511 (2018).
[96] Z. Dai, T. Senthil, and P. A. Lee, arXiv:1906.01656.
[97] M. R. Norman and J. C. S. Davis, Proc. Natl. Acad. Sci. USA **115**, 5389 (2018).
[98] S.-C. Zhang, Science **275**, 1089 (1997).
[99] H. Meier, M. Einenkel, C. Pépin, and K. B. Efetov, Phys. Rev. B **88**, 020506(R) (2013).
[100] H. Meier, C. Pépin, M. Einenkel, and K. B. Efetov, Phys. Rev. B **89**, 195115 (2014).
[101] M. Einenkel, H. Meier, C. Pépin, and K. B. Efetov, Phys. Rev. B **90**, 054511 (2014).
[102] L. E. Hayward, D. G. Hawthorn, R. G. Melko, and S. Sachdev, Science **343**, 1336 (2014).
[103] D. Chowdhury and S. Sachdev, Phys. Rev. B **90**, 134516 (2014).
[104] T. Kloss, X. Montiel, and C. Pépin, Phys. Rev. B **91**, 205124 (2015).
[105] X. Montiel, T. Kloss, and C. Pépin, Phys. Rev. B **95**, 104510 (2017).
[106] T. Kloss, X. Montiel, V. S. de Carvalho, H. Freire, and C. Pépin, Rep. Prog. Phys. **79**, 084507 (2016).
[107] C. Morice, X. Montiel, and C. Pépin, Phys. Rev. B **96**, 134511 (2017).
[108] D. Chakraborty, C. Morice, and C. Pépin, Phys. Rev. B **97**, 214501 (2018).
[109] S. Rajasekaran, J. Okamoto, L. Mathey, M. Fechner, V. Thampy, G. D. Gu, and A. Cavalleri, Science **359**, 575 (2018).
[110] W. Hu, S. Kaiser, D. Nicoletti, C. R. Hunt, I. Gierz, M. C. Hoffmann, M. Le Tacon, T. Loew, B. Keimer, and A. Cavalleri, Nat. Mater. **13**, 705 (2014).
[111] D. Fausti, R. Tobey, N. Dean, S. Kaiser, A. Dienst, M. C. Hoffmann, S. Pyon, T. Takayama, H. Takagi, and A. Cavalleri, Science **331**, 189 (2011).
[112] B. Loret, N. Auvray, Y. Gallais, M. Cazayous, A. Forget, D. Colson, M.-H. Julien, I. Paul, M. Civelli, and A. Sacuto, Nat. Phys. **15**, 771 (2019).
[113] D. Chakraborty, M. Grandadam, M. H. Hamidian, J. C. S. Davis, Y. Sidis, and C. Pépin, Phys. Rev. B **100**, 224511 (2019).
[114] J. C. Campuzano, M. R. Norman, H. Ding, M. Randeria, T. Yokoya, T. Takeuchi, T. Takahashi, T. Mochiku, K. Kadowaki, P. Guptasarma, and D. G. Hinks, Nature (London) **392**, 157 (1998).
[115] D. F. Agterberg, D. S. Melchert, and M. K. Kashyap, Phys. Rev. B **91**, 054502 (2015).
[116] M. A. Metlitski and S. Sachdev, Phys. Rev. B **82**, 075128 (2010).
[117] A. Abanov and A. V. Chubukov, Phys. Rev. Lett. **84**, 5608 (2000).
[118] A. Abanov, A. V. Chubukov, and J. Schmalian, Adv. Phys. **52**, 119 (2003).
[119] A. Abanov, A. V. Chubukov, and J. Schmalian, Europhys. Lett. **55**, 369 (2001).
[120] R. Comin, A. Frano, M. M. Yee, Y. Yoshida, H. Eisaki, E. Schierle, E. Weschke, R. Sutarto, F. He, A. Soumyanarayanan, Y. He, M. Le Tacon, I. S. Elfimov, J. E. Hoffman, G. A. Sawatzky, B. Keimer, and A. Damascelli, Science **343**, 390 (2014).
[121] Y. Wang and A. Chubukov, Phys. Rev. B **91**, 195113 (2015).
[122] A. Allais, J. Bauer, and S. Sachdev, Phys. Rev. B **90**, 155114 (2014).
[123] S. Chakravarty, R. B. Laughlin, D. K. Morr, and C. Nayak, Phys. Rev. B **63**, 094503 (2001).
[124] I. Affleck and J. B. Marston, Phys. Rev. B **37**, 3774 (1988).
[125] J. B. Marston and I. Affleck, Phys. Rev. B **39**, 11538 (1989).
[126] T. C. Hsu, J. B. Marston, and I. Affleck, Phys. Rev. B **43**, 2866 (1991).
[127] P. A. Lee, Phys. Rev. X **4**, 031017 (2014).
[128] D. Agterberg and H. Tsunetsugu, Nat. Phys. **4**, 639 (2008).
[129] R. M. Fernandes, A. V. Chubukov, J. Knolle, I. Eremin, and J. Schmalian, Phys. Rev. B **85**, 024534 (2012).
[130] A. M. Tsvelik and A. V. Chubukov, Phys. Rev. B **89**, 184515 (2014).

[131] Y. Tang, L. Mangin-Thro, A. Wildes, M. K. Chan, C. J. Dorow, J. Jeong, Y. Sidis, M. Greven, and P. Bourges, Phys. Rev. B **98**, 214418 (2018).
[132] J. Zhang, Z. Ding, C. Tan, K. Huang, O. O. Bernal, P.-C. Ho, G. D. Morris, A. D. Hillier, P. K. Biswas, S. P. Cottrell *et al.*, Sci. Adv. **4**, eaao5235 (2018).
[133] A. Pal, S. R. Dunsiger, K. Akintola, A. C. Y. Fang, A. Elhosary, M. Ishikado, H. Eisaki, and J. E. Sonier, Phys. Rev. B **97**, 060502(R) (2018).
[134] Y. Itoh, T. Machi, and A. Yamamoto, Phys. Rev. B **95**, 094501 (2017).
[135] V. Balédent, D. Haug, Y. Sidis, V. Hinkov, C. T. Lin, and P. Bourges, Phys. Rev. B **83**, 104504 (2011).